Generative Adversarial Networks, Flow Matching, Diffusion Models

Milan Straka

May 6, 2025

Charles University
ÚFAL
LANGTECH
EUROPEAN UNION
European Structural and Investment Fund
Operational Programme Research, Development and Education

Charles University in Prague
Faculty of Mathematics and Physics
Institute of Formal and Applied Linguistics

Generative Models

Generative Models

There are several approaches how to represent a probability distribution $P(\mathbf{x})$. **Likelihood-based models** represent the probability density function directly, often using an unnormalized probabilistic model (also called energy-based model; i.e., specifying a non-zero *score* or *density* or *logits*):

$$P_{\boldsymbol{\theta}}(\mathbf{x}) = \frac{e^{f_{\boldsymbol{\theta}}(\mathbf{x})}}{Z_{\boldsymbol{\theta}}}.$$

However, estimating the normalization constant $Z_{\boldsymbol{\theta}} = \int e^{f_{\boldsymbol{\theta}}(\mathbf{x})}\,\mathrm{d}\mathbf{x}$ is often intractable.

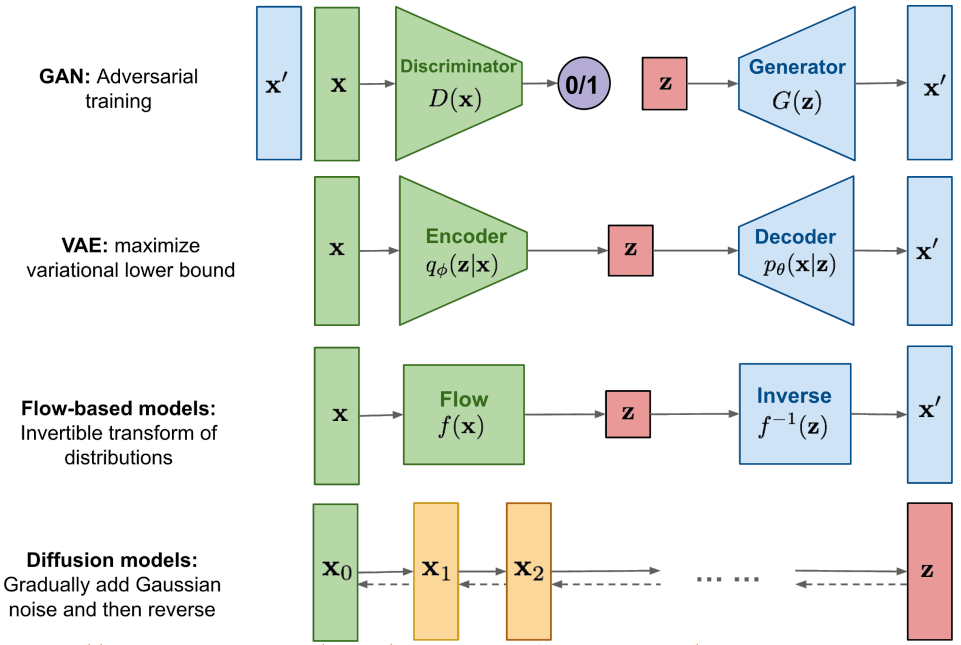

https://lilianweng.github.io/posts/2021-07-11-diffusion-models/generative-overview.png

- We can compute $Z_{\boldsymbol{\theta}}$ by restricting the model architecture (sequence modeling, invertible networks in normalizing flows);
- we can only approximate it (using for example variational inference as in VAE);
- we can use **implicit generative models**, which avoid representing likelihood (like GANs).

Generative Adversarial Networks

Generative Adversarial Networks

We have a **generator** $G(\boldsymbol{z}; \boldsymbol{\theta}_g)$, which given $\boldsymbol{z} \sim P(\mathbf{z})$ generates data $\boldsymbol{x}$.

Then we have a **discriminator** $D(\boldsymbol{x}; \boldsymbol{\theta}_d)$, which given data $\boldsymbol{x}$ generates a probability whether $\boldsymbol{x}$ comes from real data or is generated by a generator.

The discriminator and generator play the following game:

$$\min_G \max_D \mathbb{E}_{\boldsymbol{x} \sim P_{\text{data}}} [\log D(\boldsymbol{x})] + \mathbb{E}_{\boldsymbol{z} \sim P(\mathbf{z})} [\log(1 - D(G(\boldsymbol{z})))].$$

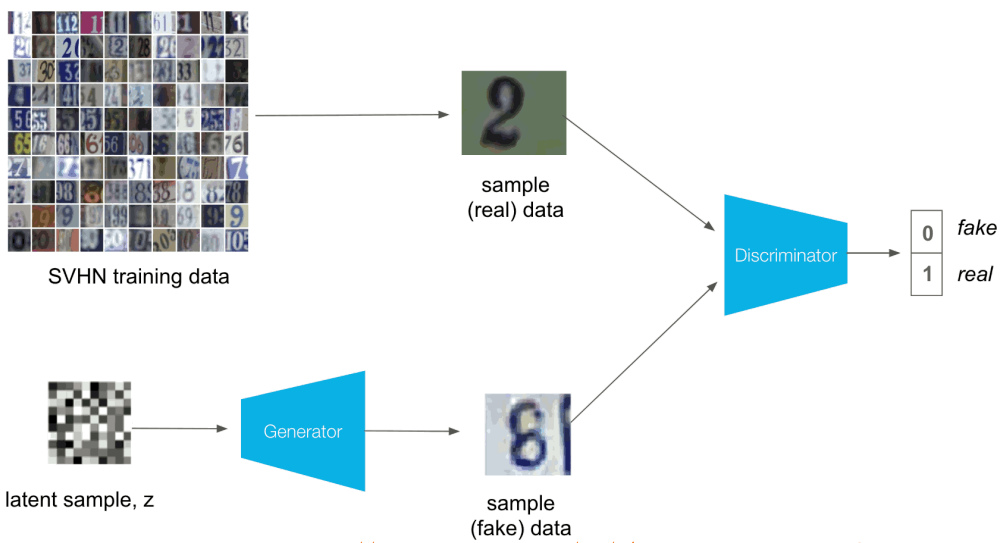

https://miro.medium.com/v2/1*-ucVYsbDnwa2NM-f5qm_Yg.png

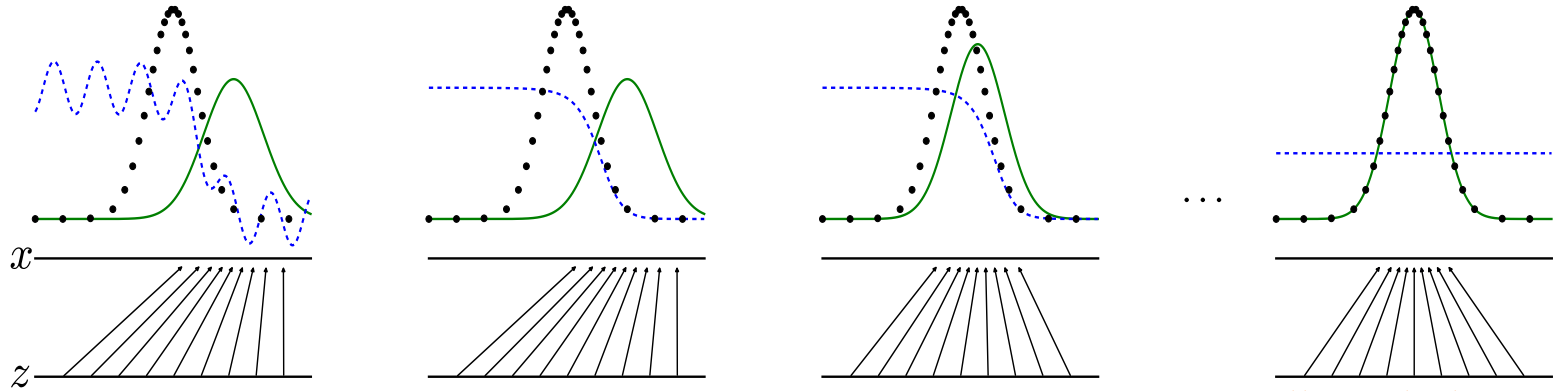

Figure 1 of "Generative Adversarial Nets", https://arxiv.org/abs/1406.2661

The generator and discriminator are alternately trained, the discriminator by

$$\arg\max_{\boldsymbol{\theta}_d} \mathbb{E}_{\boldsymbol{x}\sim P_{\text{data}}}[\log D(\boldsymbol{x})] + \mathbb{E}_{\boldsymbol{z}\sim P(\mathbf{z})}[\log(1 - D(G(\boldsymbol{z})))]$$

and the generator by

$$\arg\min_{\boldsymbol{\theta}_g} \mathbb{E}_{\boldsymbol{z}\sim P(\mathbf{z})}[\log(1 - D(G(\boldsymbol{z})))].$$

Basically, the discriminator acts as a trainable loss for the generator.

Because $\log(1 - D(G(\boldsymbol{z})))$ can saturate at the beginning of the training, where the discriminator can easily distinguish real and generated samples, the generator can be trained by

$$\arg\min_{\boldsymbol{\theta}_g} \mathbb{E}_{\boldsymbol{z} \sim P(\mathbf{z})}[-\log D(G(\boldsymbol{z}))]$$

instead, which results in the same fixed-point dynamics, but much stronger gradients early in learning.

On top of that, if you train the generator by using "real" as the gold label of the discriminator, you naturally get the above loss (which is the negative log likelihood, contrary to the original formulation).

Algorithm 1 Minibatch stochastic gradient descent training of generative adversarial nets. The number of steps to apply to the discriminator, k, is a hyperparameter. We used $k = 1$, the least expensive option, in our experiments.

for number of training iterations **do**

for k steps **do**

- Sample minibatch of m noise samples $\{\boldsymbol{z}^{(1)}, \ldots, \boldsymbol{z}^{(m)}\}$ from noise prior $p_g(\boldsymbol{z})$.
- Sample minibatch of m examples $\{\boldsymbol{x}^{(1)}, \ldots, \boldsymbol{x}^{(m)}\}$ from data generating distribution $p_{\text{data}}(\boldsymbol{x})$.
- Update the discriminator by ascending its stochastic gradient:

$$\nabla_{\theta_d} \frac{1}{m} \sum_{i=1}^{m} \left[\log D\left(\boldsymbol{x}^{(i)}\right) + \log\left(1 - D\left(G\left(\boldsymbol{z}^{(i)}\right)\right)\right) \right].$$

end for

- Sample minibatch of m noise samples $\{\boldsymbol{z}^{(1)}, \ldots, \boldsymbol{z}^{(m)}\}$ from noise prior $p_g(\boldsymbol{z})$.
- Update the generator by descending its stochastic gradient:

$$\nabla_{\theta_g} \frac{1}{m} \sum_{i=1}^{m} \log\left(1 - D\left(G\left(\boldsymbol{z}^{(i)}\right)\right)\right).$$

end for

The gradient-based updates can use any standard gradient-based learning rule. We used momentum in our experiments.

Algorithm 1 of "Generative Adversarial Nets", https://arxiv.org/abs/1406.2661

Generative Adversarial Networks

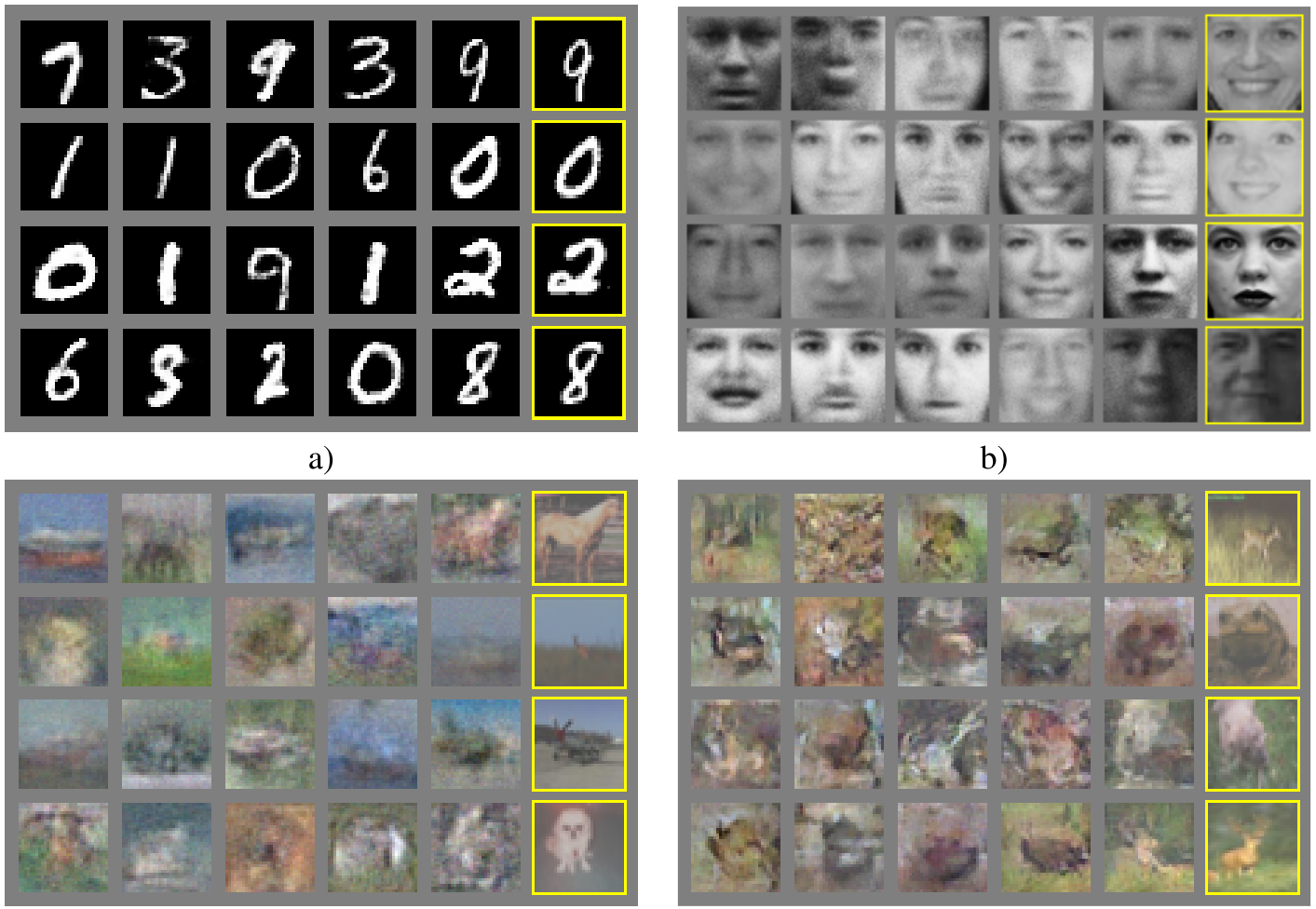

Figure 2 of "Generative Adversarial Nets", https://arxiv.org/abs/1406.2661

Conditional GAN

Assuming our dataset is conditional, i.e., the individual examples are pairs $(\boldsymbol{x}, y)$ with y being the image class, GANs can be easily extended to allow conditioning:

- the generator gets y as an additional input: $G(\boldsymbol{z}, y)$,
- the discriminator also gets y as an additional input: $D(\boldsymbol{x}, y)$.

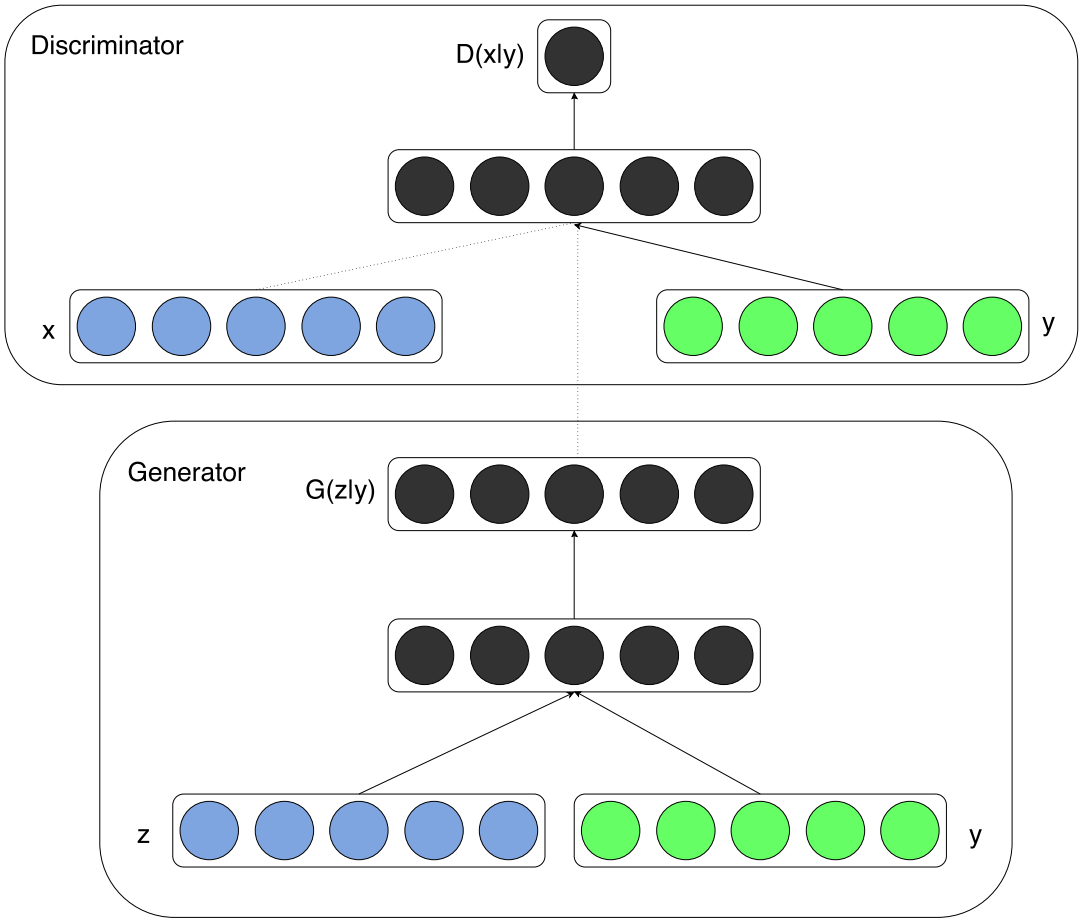

Figure 1 of "Conditional Generative Adversarial Nets", https://arxiv.org/abs/1411.1784

Deep Convolutional GAN

In Deep Convolutional GAN, the discriminator is a convolutional network (with batch normalization) and the generator is also a convolutional network, utilizing transposed convolutions.

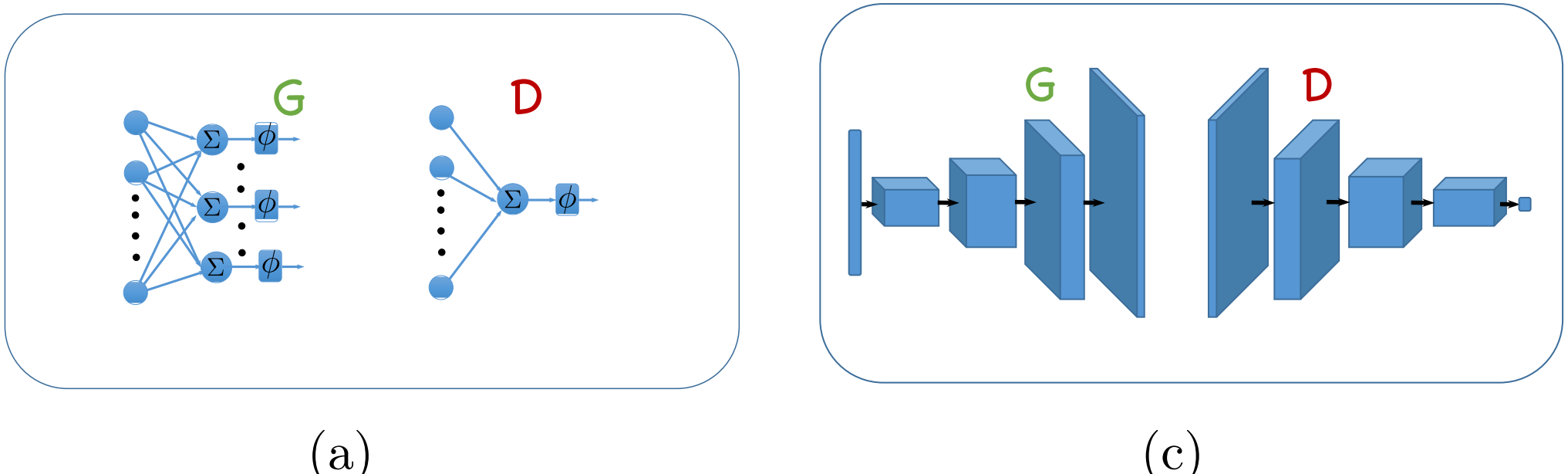

Figure 1 of "An Online Learning Approach to Generative Adversarial Networks", https://arxiv.org/abs/1706.03269

Deep Convolutional GAN

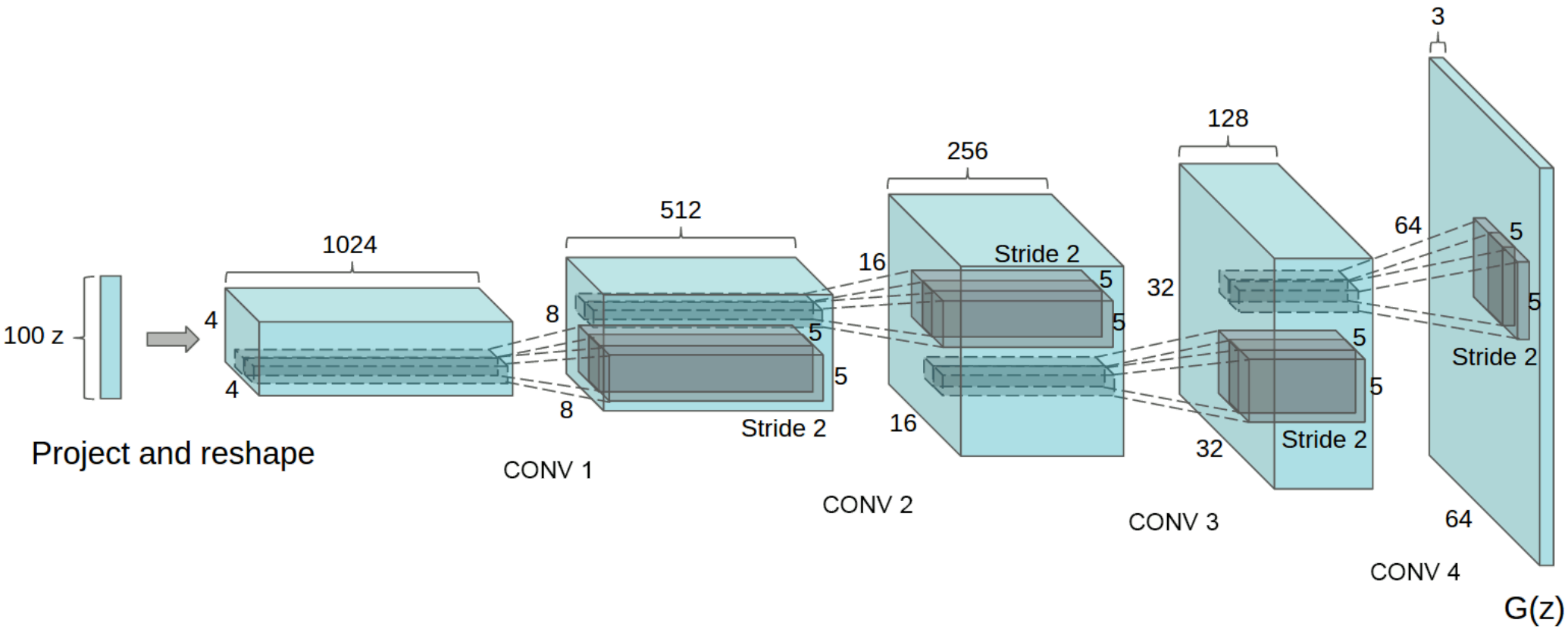

Figure 1 of "Unsupervised Representation Learning with Deep Convolutional Generative Adversarial Networks", https://arxiv.org/abs/1511.06434

Deep Convolutional GAN

Figure 3 of "Unsupervised Representation Learning with Deep Convolutional Generative Adversarial Networks", https://arxiv.org/abs/1511.06434

Deep Convolutional GAN

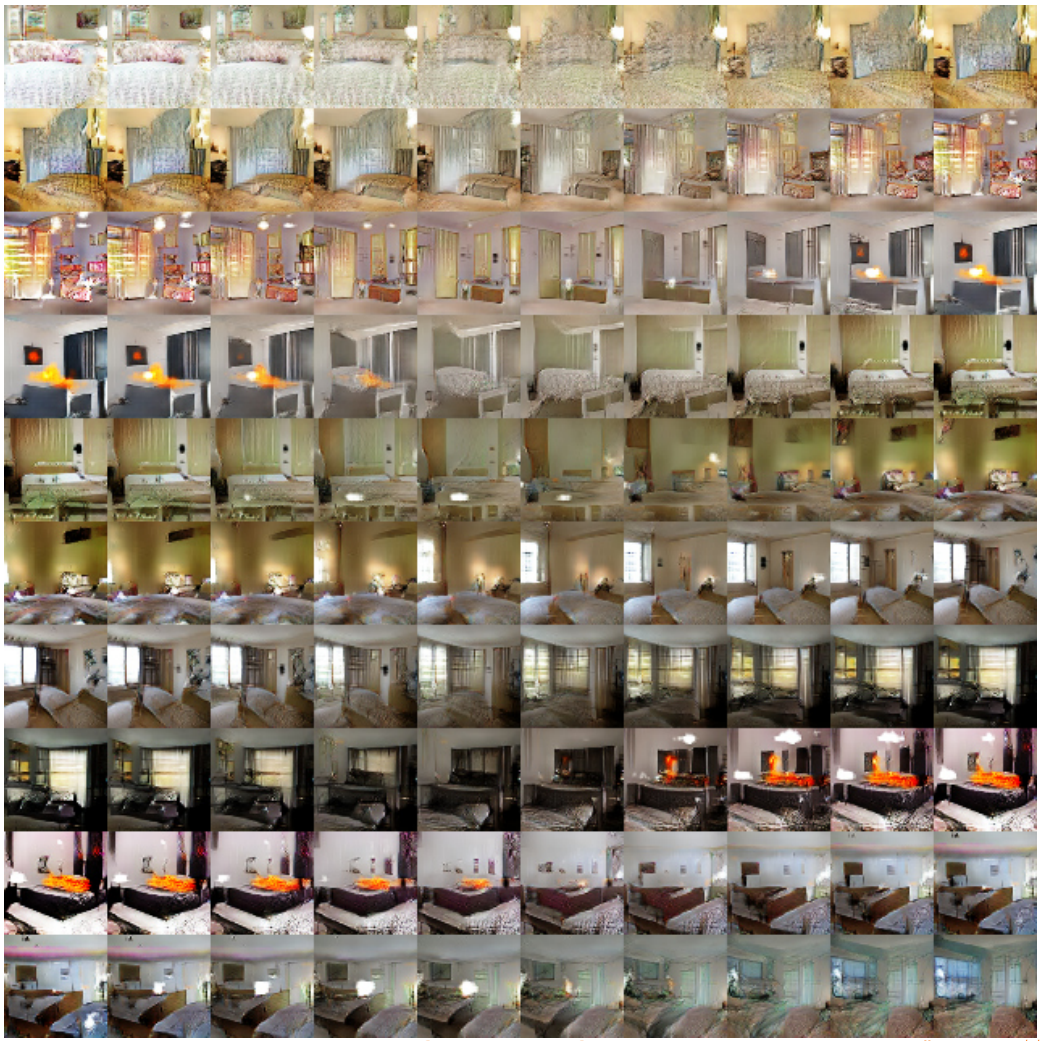

Figure 4 of "Unsupervised Representation Learning with Deep Convolutional Generative Adversarial Networks", https://arxiv.org/abs/1511.06434

Deep Convolutional GAN

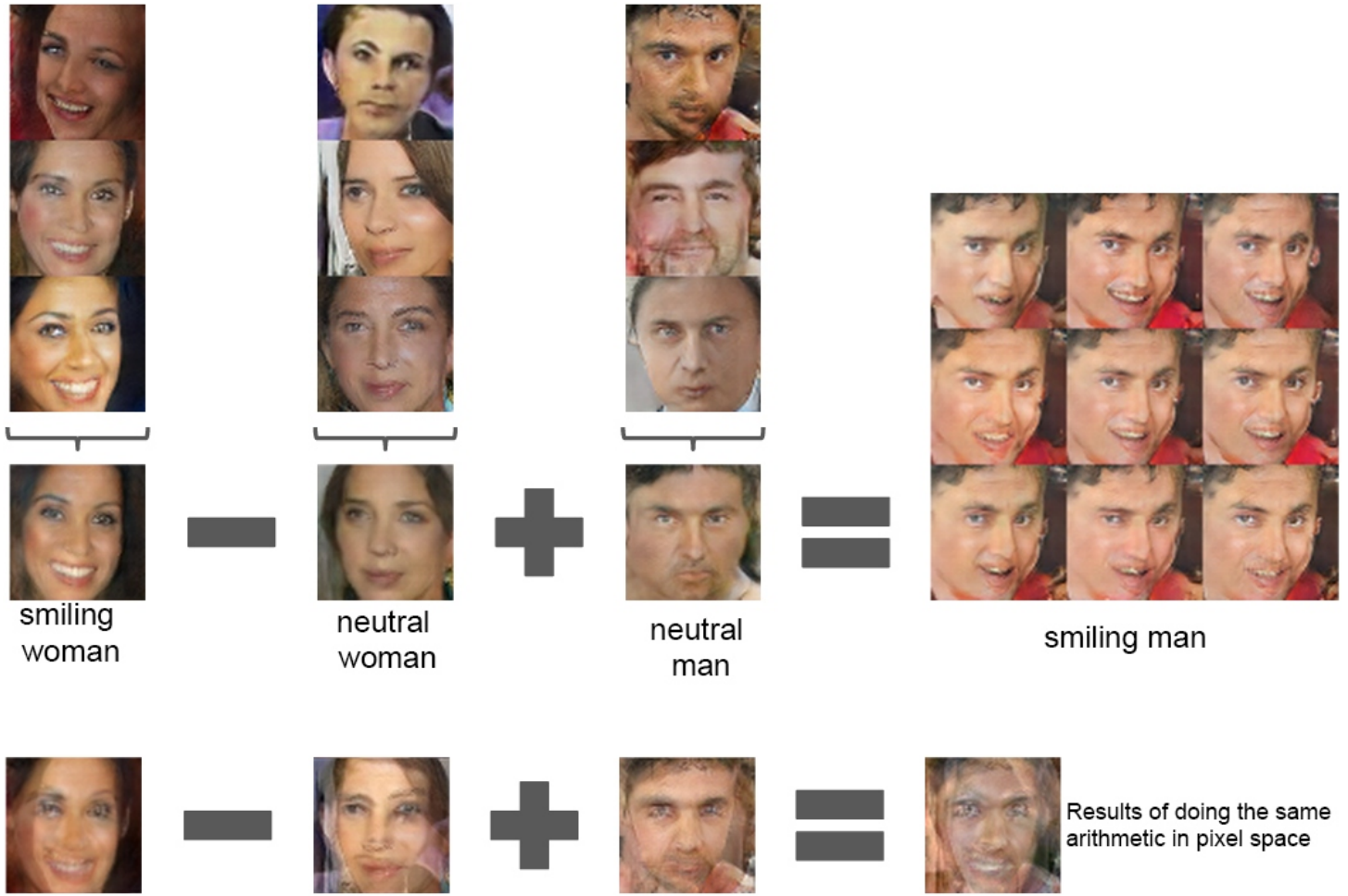

Figure 7 of "Unsupervised Representation Learning with Deep Convolutional Generative Adversarial Networks", https://arxiv.org/abs/1511.06434

Deep Convolutional GAN

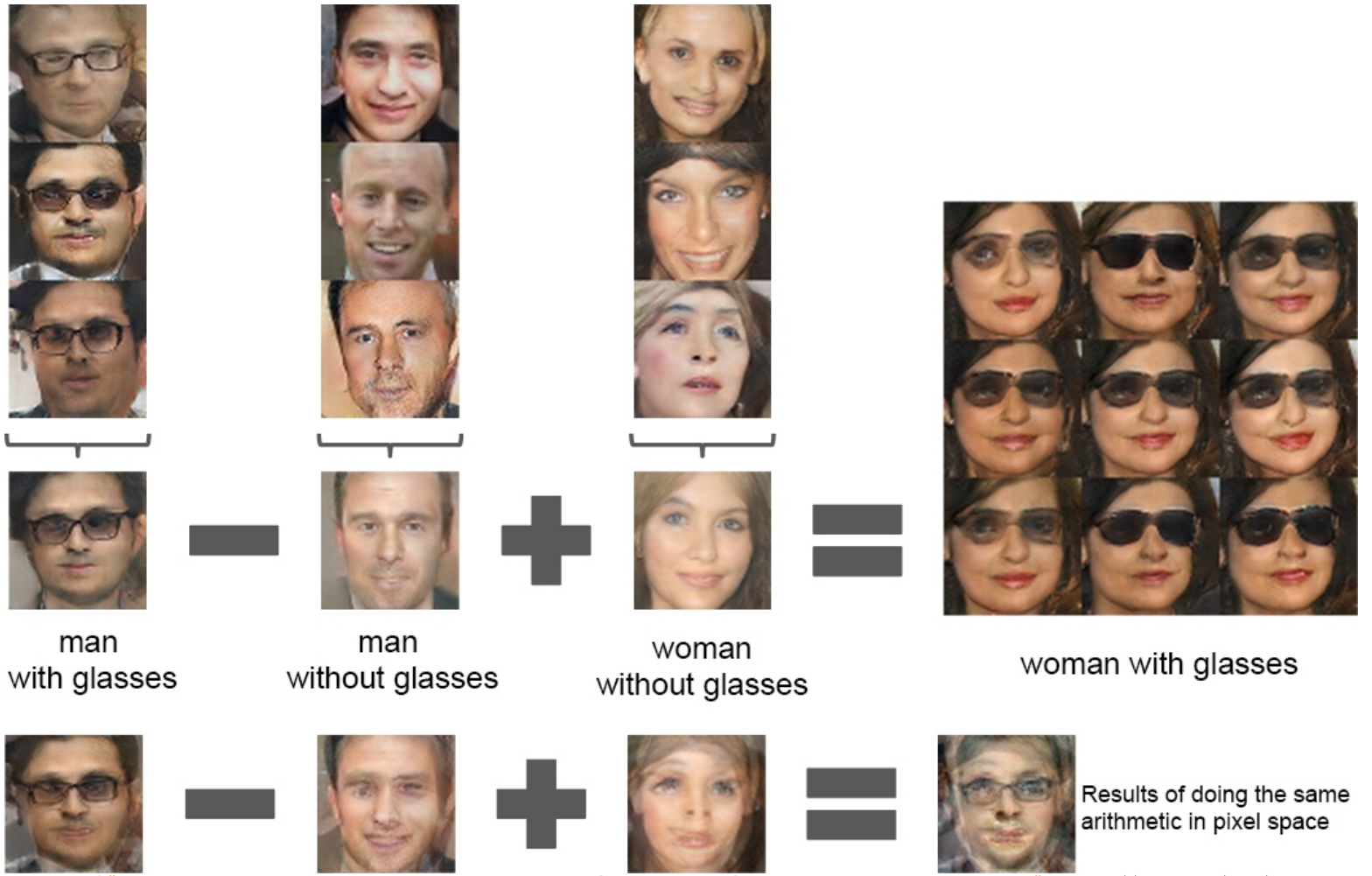

Figure 7 of "Unsupervised Representation Learning with Deep Convolutional Generative Adversarial Networks", https://arxiv.org/abs/1511.06434

Deep Convolutional GAN

Figure 8 of "Unsupervised Representation Learning with Deep Convolutional Generative Adversarial Networks", https://arxiv.org/abs/1511.06434

https://miro.medium.com/max/1400/1*r8cuSIaM5oHUERP01TCTxg.jpeg

GANs Training – Results of In-House BigGAN Training

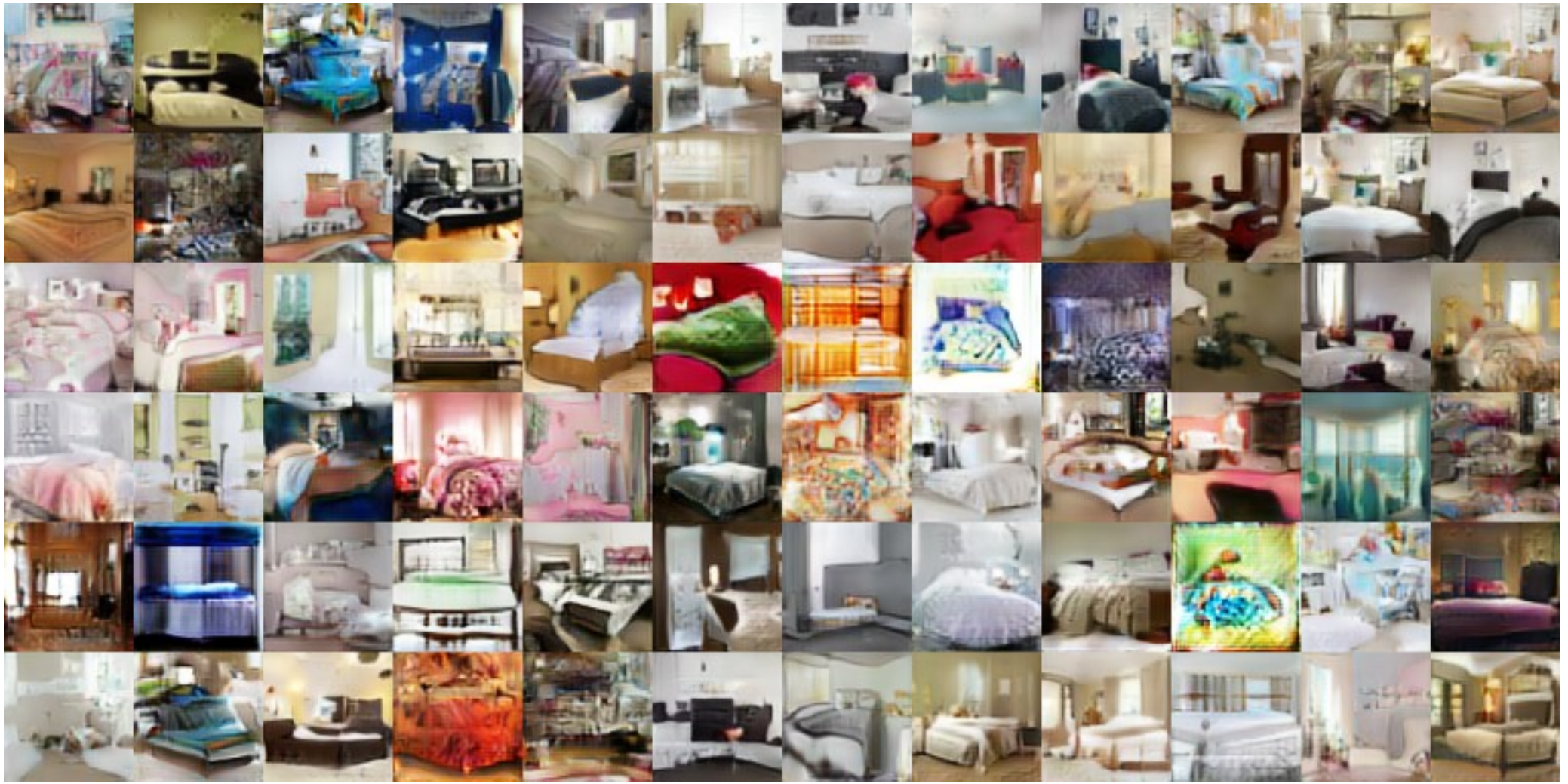

GANs are Problematic to Train

GANs are Problematic to Train

Unfortunately, alternating SGD steps are not guaranteed to reach even a local optimum of a minimax problem, consider the following one:

$$\min_x \max_y x \cdot y.$$

The update rules of x and y for learning rate α are

$$\begin{bmatrix} x_{n+1} \\ y_{n+1} \end{bmatrix} = \begin{bmatrix} 1 & -\alpha \\ \alpha & 1 \end{bmatrix} \begin{bmatrix} x_n \\ y_n \end{bmatrix}.$$

The update matrix is a rotation matrix multiplied by a constant $\sqrt{1+\alpha^2} > 1$

$$\begin{bmatrix} 1 & -\alpha \\ \alpha & 1 \end{bmatrix} = \sqrt{1+\alpha^2} \cdot \begin{bmatrix} \cos\varphi & -\sin\varphi \\ \sin\varphi & \cos\varphi \end{bmatrix},$$

so the SGD will not converge with arbitrarily small step size.

GANs are Problematic to Train

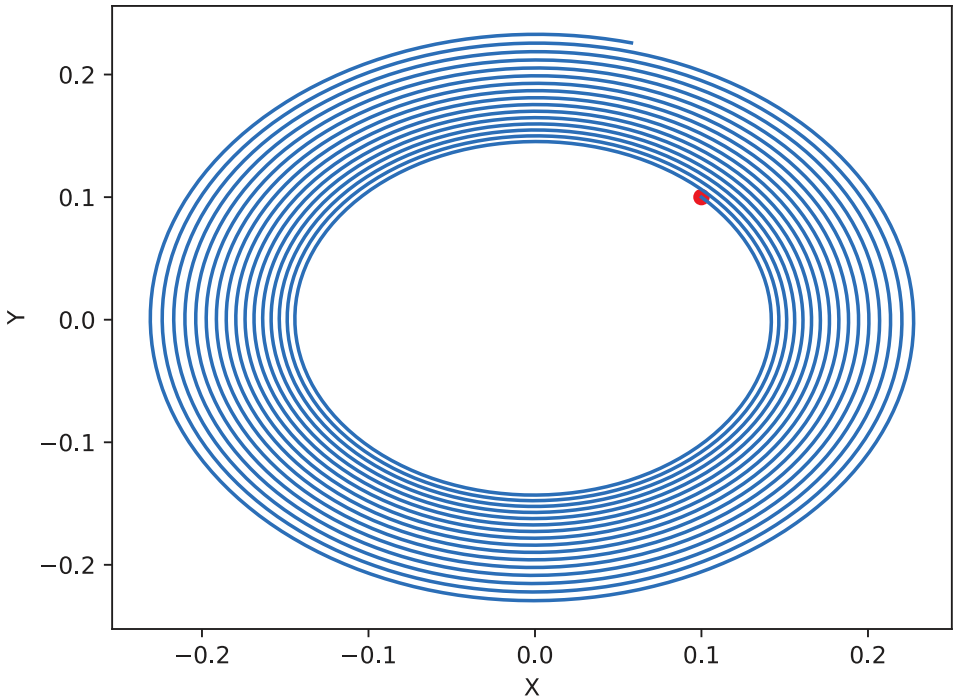

(a)

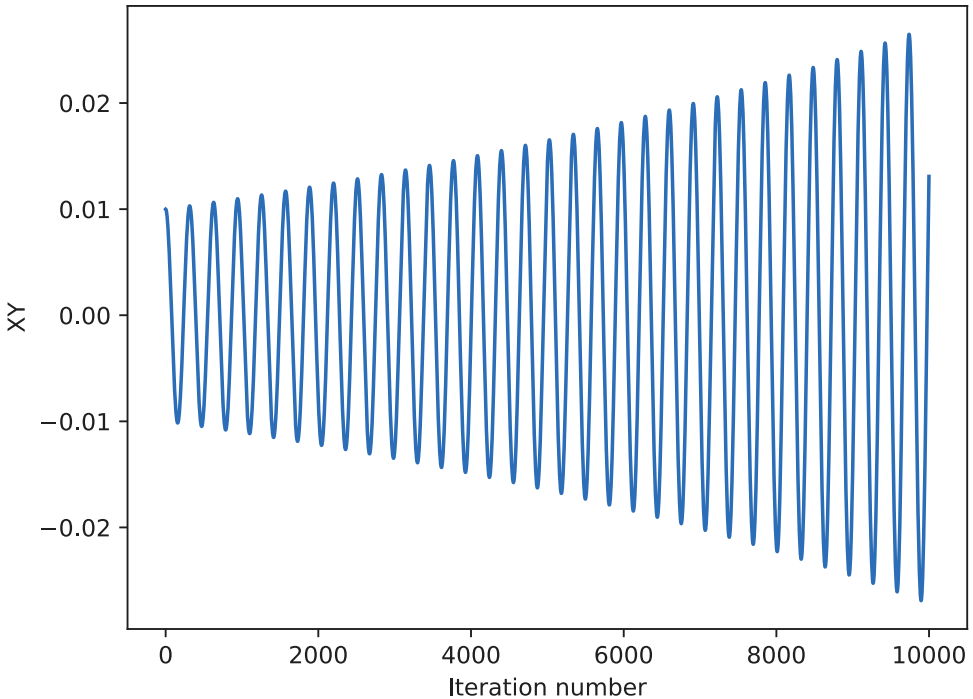

(b)

Fig. 1: Performance of gradient method with fixed step size for Example 2. (a) illustrates the choices of x and y as iteration processes, the red point $(0.1, 0.1)$ is the initial value. (b) illustrates the value of xy as a function of iteration numbers.

Figure 1 of "Fictitious GAN: Training GANs with Historical Models", https://arxiv.org/abs/1803.08647

GANs are Problematic to Train

- GANs suffer from "mode collapse"

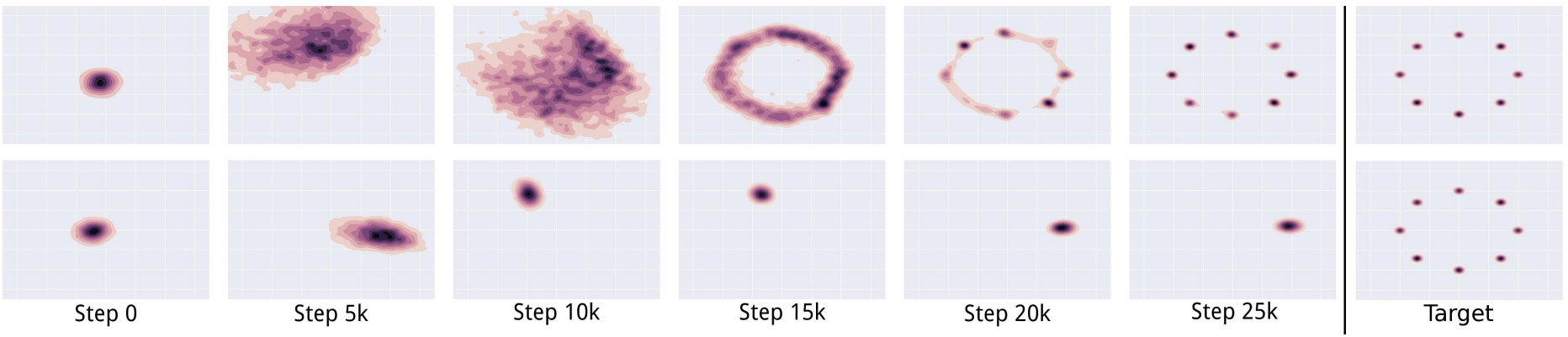

Figure 2 of "Unrolled Generative Adversarial Networks", https://arxiv.org/abs/1611.02163

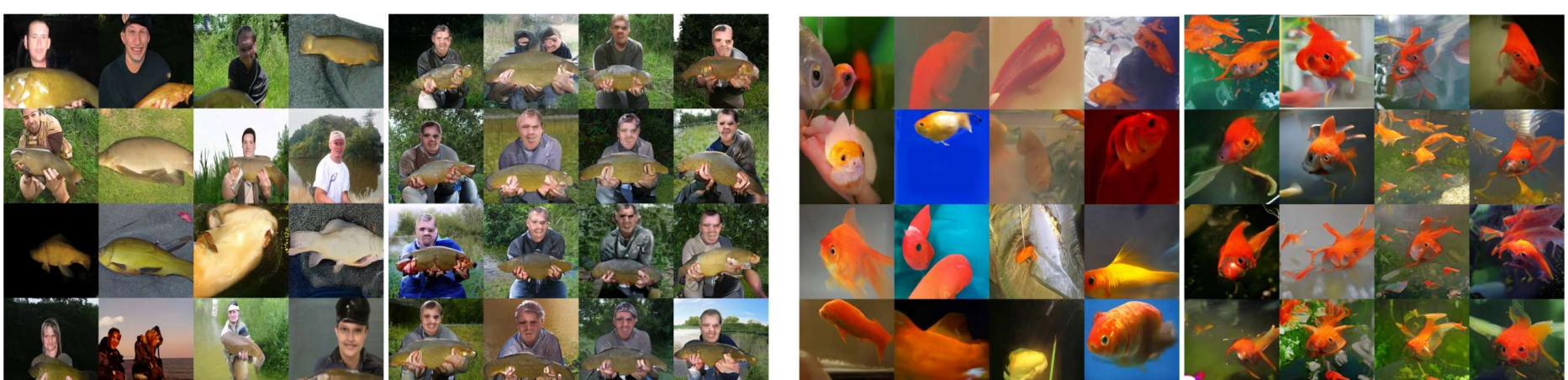

Figure 5 of "Generating Diverse High-Fidelity Images with VQ-VAE-2", https://arxiv.org/abs/1906.00446

GANs are Problematic to Train

The training can be improved by various tricks:

- If the discriminator could see the whole batch, similar samples in it would be candidates for fake images.
  - Batch normalization helps a lot with this.
- Unrolling the discriminator update helps generator to consider not just the current discriminator, but also how the future versions would react to the generator outputs. (The discriminator training is unchanged.)

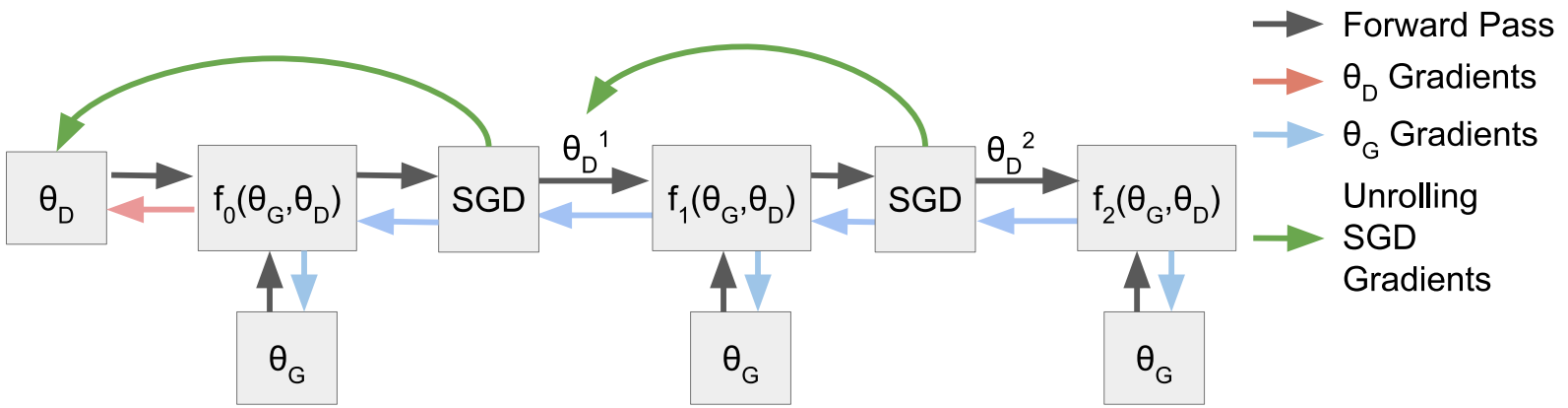

Figure 1 of "Unrolled Generative Adversarial Networks", https://arxiv.org/abs/1611.02163

- Many others, like Wasserstein GAN, spectral normalization, progressive growing, ...

Comparison of VAEs and GANs

The Variational Autoencoders:

- are theoretically-pleasing;
- also provide an encoder, so apart from generation, they can be used as unsupervised feature extraction (the VAE encoder is used in various modeling architectures);
- the generated samples tend to be blurry, especially with L^1 or L^2 loss (because of the sampling used in the reconstruction; patch-based discriminator with perceptual loss helps).

The Generative Adversarial Networks:

- offer high sample quality;
- are difficult to train and suffer from mode collapse.

In past few years, GANs saw a big development, improving the sample quality substantially. However, since 2019/2020, VAEs have shown remarkable progress (alleviating the blurriness issue by using perceptual loss and a 2D grid of latent variables), and are being used for generation too. Furthermore, additional approaches (normalizing flows, diffusion models) were also being explored, with diffusion models becoming the most promising approach since Q2 of 2021, surpassing both VAEs and GANs.

Flow Matching

Flow Matching

In the past years (since 2022), the dominant approach for generating images has been based on **diffusion models** (used by Stable Diffusion, DALL-E, ...).

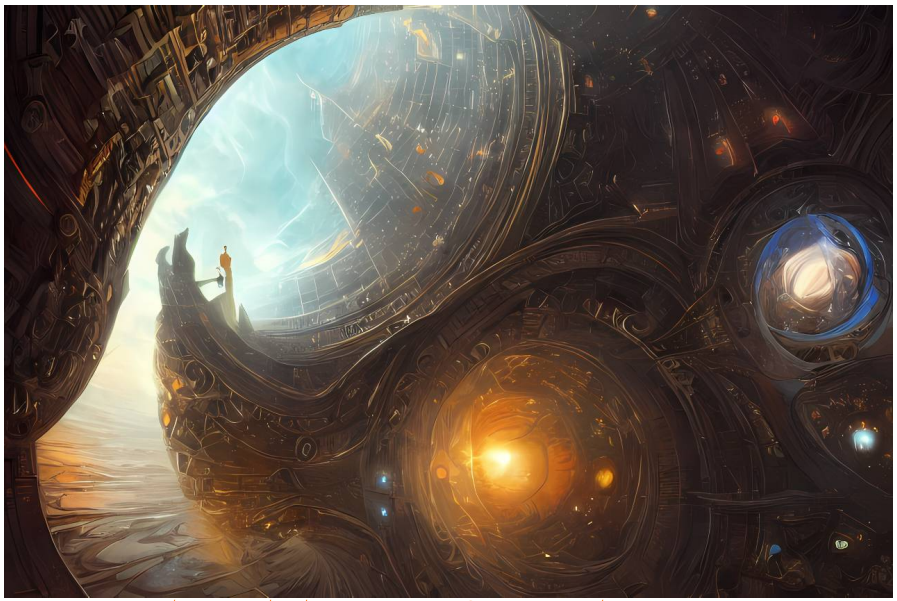

https://images.squarespace-cdn.com/content/v1/6213c340453c3f502425776e/0715034d-4044-4c55-9131-e4bfd6dd20ca/2_4x.png

The diffusion models are deeply connected to **score-based generative models**, which were developed independently, but are just a different perspective on the same model family.

Recently, **conditional flow matching** was proposed as a generalization of both these approaches, and that is the method we will describe in most detail.

Generative Modeling

The general framework of generative modeling assumes we have samples $\boldsymbol{x}^{(1)}, \boldsymbol{x}^{(2)}, \ldots, \boldsymbol{x}^{(N)}$ from the data generating distribution p_{data}, and the main challenges we should overcome are:

- provide fast sampling (diffusion models were originally not great here),
- generate high-quality samples (VAE struggles with this goal),
- properly cover the density of p_{data} (the main issue of GANs).

Modern approach to generative modeling is to start with a simple base distribution p_0, usually a standard Gaussian $\mathcal{N}(\mathbf{0}, \boldsymbol{I})$, and learn a mapping that transforms that distribution into p_{data}.

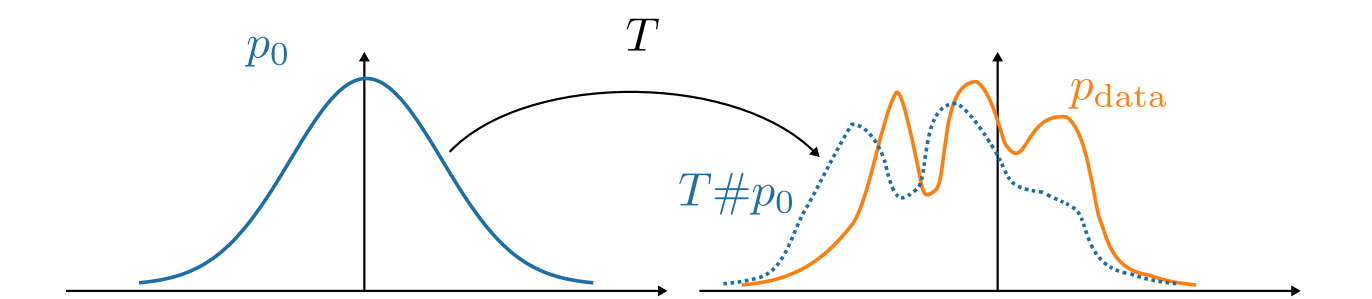

https://dl.heeere.com/conditional-flow-matching/assets/img/2025-04-28-conditional-flow-matching/T_theta_pushforward.svg

Sampling then can be performed by sampling from p_0 and performing the transformation.

Generating Images From Standard Normal Base Distribution

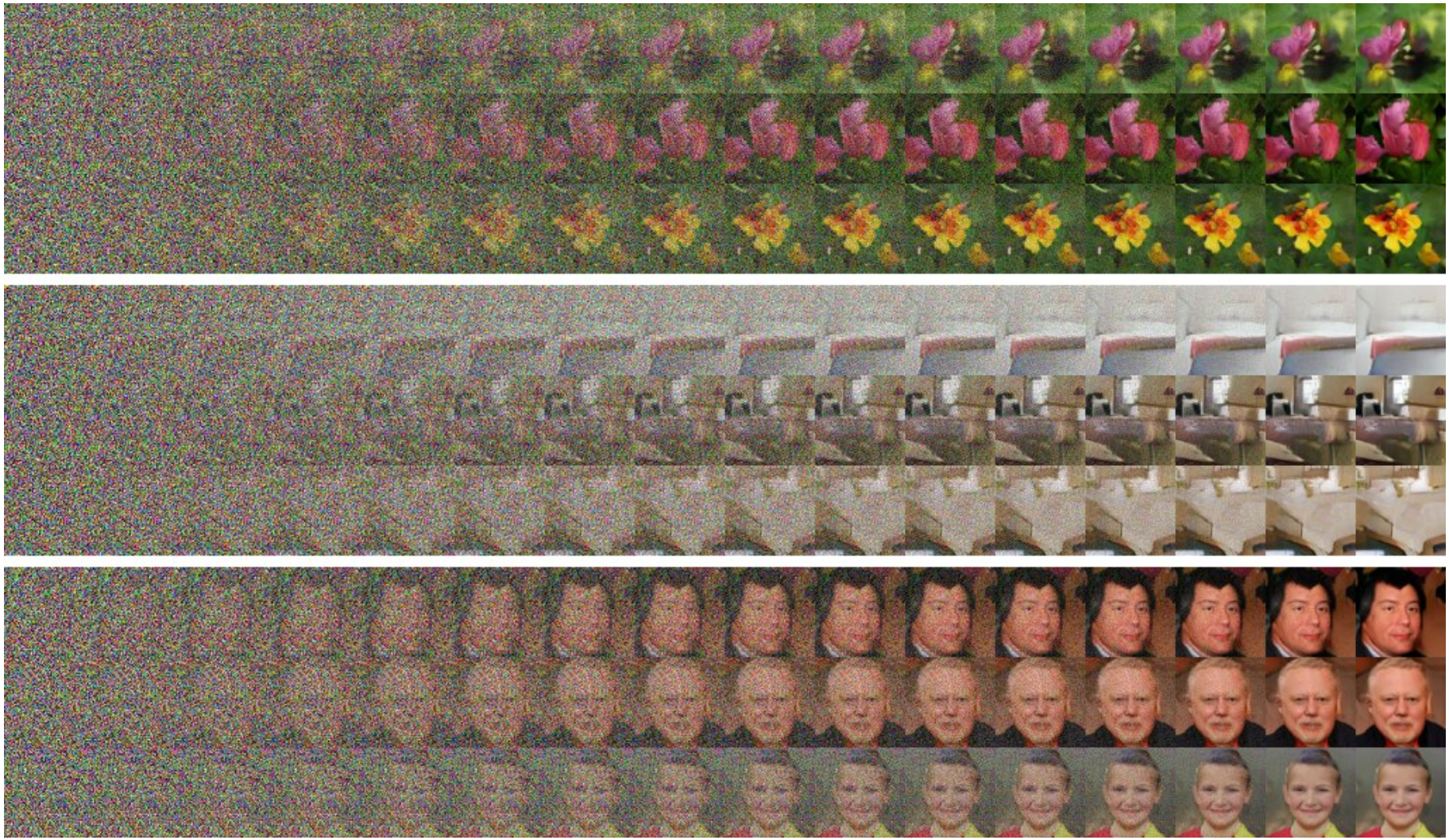

Flow Matching

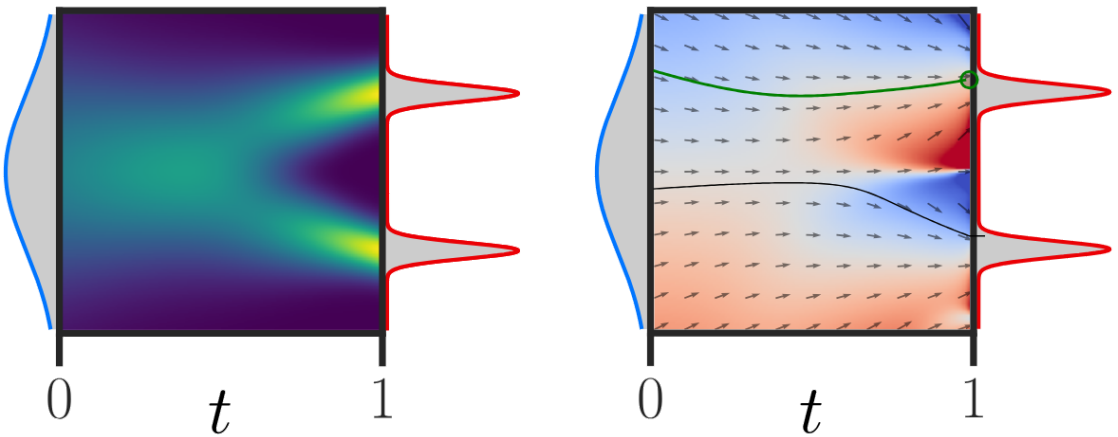

https://dl.heeere.com/conditional-flow-matching/blog/conditional-flow-matching/

The important concepts used by flow matching are:

- the **probability density path** $p : [0,1] \times \mathbb{R}^d \to \mathbb{R}_{>0}$, which is a time-dependent probability density function, i.e., $\int p_t(\boldsymbol{x})\,\mathrm{d}\boldsymbol{x} = 1$;
  - this probability density path should transform the prior p_0 into $p_1 = p_{\text{data}}$
- a **time-dependent vector field** $u : [0,1] \times \mathbb{R}^d \to \mathbb{R}^d$, which can be used to construct a **flow** $\varphi : [0,1] \times \mathbb{R}^d \to \mathbb{R}^d$ via an ordinary differential equation:

$$\frac{d}{dt}\varphi_t(\boldsymbol{x}) = u_t(\varphi_t(\boldsymbol{x})), \quad \varphi_0(\boldsymbol{x}) = \boldsymbol{x}.$$

Flow Matching

Note that the solution of the flow ODE

$$\frac{d}{dt}\varphi_t(\boldsymbol{x}) = u_t(\varphi_t(\boldsymbol{x})), \quad \varphi_0(\boldsymbol{x}) = \boldsymbol{x}$$

is unique when u_t is Lipschitz continuous in $\boldsymbol{x}$ and continuous in t (Picard–Lindelöf theorem).

Recall that in a residual network, we update the current value by adding the result of a residual block

$$\boldsymbol{h}_{t+1} = \boldsymbol{h}_t + f(\boldsymbol{h}_t; \boldsymbol{\theta}_t),$$

which we can also write as

$$\boldsymbol{h}_{t+1} - \boldsymbol{h}_t = f(\boldsymbol{h}_t; \boldsymbol{\theta}_t),$$

where we can interpret the residual block as a "discrete derivative".

Therefore, the flow can be considered to be a continuous generalization of residual networks.

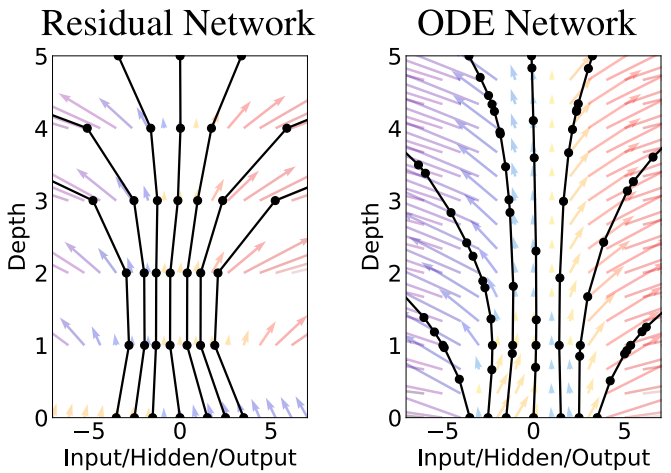

Figure 1: *Left:* A Residual network defines a discrete sequence of finite transformations. *Right:* A ODE network defines a vector field, which continuously transforms the state. *Both:* Circles represent evaluation locations.

Figure 1 of "Neural Ordinary Differential Equations", https://arxiv.org/abs/1806.07366

Flow Matching: Transport Equation

A vector field u_t is said to **generate** a probability density path p_t if the *transport equation* holds:

$$\frac{d}{dt}p_t(\boldsymbol{x}) = -\operatorname{div}\left(p_t(\boldsymbol{x})u_t(\boldsymbol{x})\right),$$

where the **divergence** $\operatorname{div}(\boldsymbol{z}) \stackrel{\text{def}}{=} \sum_i \frac{\partial z_i}{\partial x_i}$ is a vector operator that operates on a vector field, producing for every point a scalar value, the field's *source* at that point (a positive value means a point is a source; negative if it is a sink).

The $p_t(\boldsymbol{x})u_t(\boldsymbol{x})$ is a *flux*, the probability mass passing through every point of the space (in the direction of the vector field).

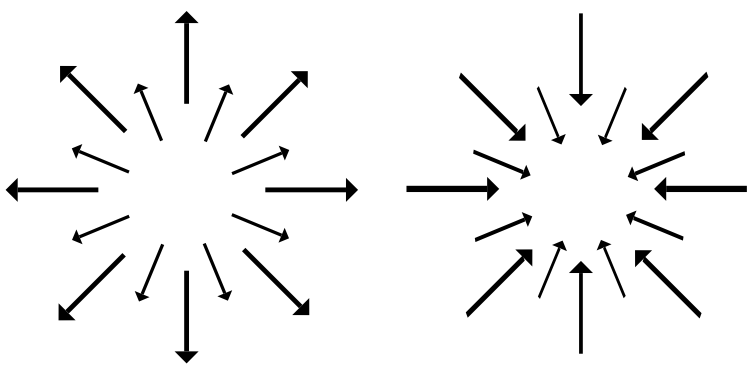

https://upload.wikimedia.org/wikipedia/commons/e/ee/Divergence_(captions).svg

Flow Matching: Basic Objective

Assume we have a base distribution p_0, usually $\mathcal{N}(\mathbf{0}, \boldsymbol{I})$, and samples $\boldsymbol{x}^{(i)}$ of the data generating distribution $p_1 = p_{\text{data}}$. Given a target probability density path p_t and a corresponding vector field u_t generating p_t, the *flow matching (FM) objective* is

$$\mathcal{L}_{\text{FM}}(\boldsymbol{\theta}) \stackrel{\text{def}}{=} \mathbb{E}_{t, p_t(\boldsymbol{x})} \left\| v_t(\boldsymbol{x}; \boldsymbol{\theta}) - u_t(\boldsymbol{x}) \right\|^2.$$

However, we need to overcome that we have no prior knowledge on how the p_t and u_t should look like given that there are many possible probability density paths p_t, and that for an arbitrary p_t, we usually do not have access to the closed form of its generating vector field u_t.

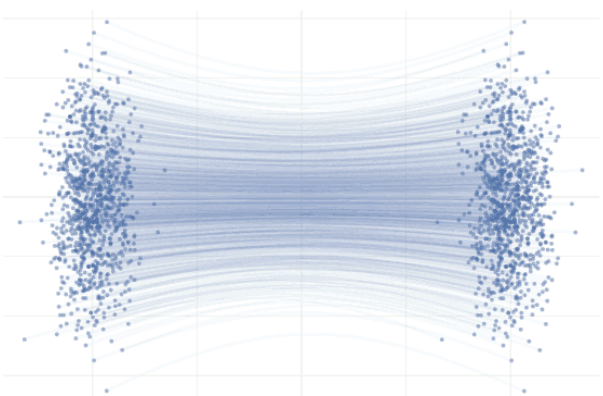

https://mlg.eng.cam.ac.uk/blog/2024/01/20/flow-matching.html

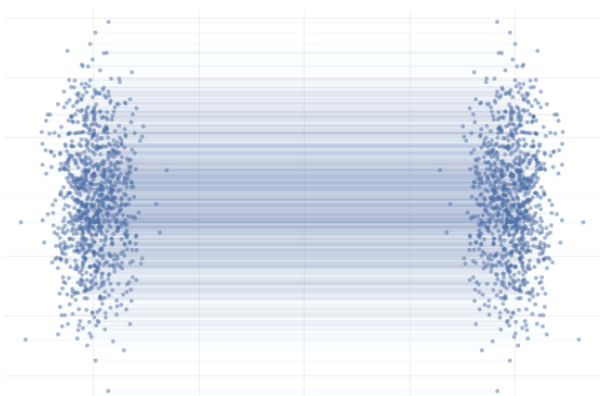

https://mlg.eng.cam.ac.uk/blog/2024/01/20/flow-matching.html

Flow Matching: Basic Overview

Once we solve the remaining issues with the flow matching objective, we train a NN model $v_t(\boldsymbol{x}; \boldsymbol{\theta})$ by predicting (matching) the vector field $u_t(\boldsymbol{x})$.

Usually, the UNet architecture with skip connections is used to model v_t.

Training

During training, we minimize an objective corresponding to flow matching

$$\mathcal{L}_{\mathrm{FM}}(\boldsymbol{\theta}) \stackrel{\mathrm{def}}{=} \mathbb{E}_{t, p_t(\boldsymbol{x})} \left\| v_t(\boldsymbol{x}; \boldsymbol{\theta}) - u_t(\boldsymbol{x}) \right\|^2,$$

i.e., by performing a regression on the vector predicted by the model v_t.

Sampling

In order to generate an image, we start by sampling $\mathbf{x}_0 \sim p_0$, and then perform numerical integration by the Euler method using T steps by

$$\boldsymbol{x}_{t+1/T} \leftarrow \boldsymbol{x}_t + \frac{1}{T} v_t(\boldsymbol{x}_t; \boldsymbol{\theta}).$$

More involved methods like the midpoint or Runge-Kutta can also be used.

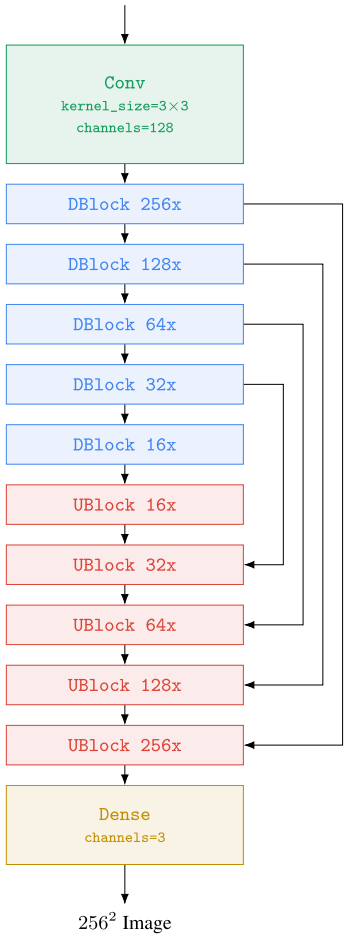

Figure A.30 of "Photorealistic Text-to-Image Diffusion Models with Deep Language Understanding", https://arxiv.org/abs/2205.11487

Conditional Flow Matching

Conditional and Marginal Probability Paths

Instead of directly defining the probability density path, we can construct it as a mixture of simpler probability paths. Together with the fact that we do not have direct access to the data generating distribution $p_1 = p_{\text{data}}$ apart from its samples, we turn to **conditional probability paths** $p_t(\boldsymbol{x}|\boldsymbol{x}_1)$, which we design so that

- $p_0(\boldsymbol{x}|\boldsymbol{x}_t) = p_0(\boldsymbol{x})$,
- $p_1(\boldsymbol{x}|\boldsymbol{x}_1)$ is tightly concentrated around $\boldsymbol{x}_1$, for example by using a normal distribution with a small variance $\sigma^2_{\text{min}} > 0$:

$$p_1(\boldsymbol{x}|\boldsymbol{x}_1) = \mathcal{N}(\boldsymbol{x}|\boldsymbol{x}_1, \sigma^2_{\text{min}}\boldsymbol{I}).$$

We can then define the *marginal probability path* as

$$p_t(\boldsymbol{x}) \overset{\text{def}}{=} \mathbb{E}_{\boldsymbol{x}_1 \sim p_{\text{data}}}\left[p_t(\boldsymbol{x}|\boldsymbol{x}_1)\right] = \int p_t(\boldsymbol{x}|\boldsymbol{x}_1) p_{\text{data}}(\boldsymbol{x}_1)\,\mathrm{d}\boldsymbol{x}_1.$$

Because we defined the conditional probability paths to concentrate tightly around $\boldsymbol{x}_1$, the marginal probability $p_1(\boldsymbol{x}) \approx p_{\text{data}}$.

Conditional and Marginal Vector Fields

Analogously to how we defined the marginal probability path using the conditional probability paths, it is also possible to define the *marginal vector field* (the vector field of the marginal probability path) using the *conditional vector fields* $u_t(\boldsymbol{x}|\boldsymbol{x}_1)$ (the vector fields of the conditional probability paths):

$$u_t(\boldsymbol{x}) \stackrel{\text{def}}{=} \mathbb{E}_{\boldsymbol{x}_1 \sim p_{\text{data}}}\left[u_t(\boldsymbol{x}|\boldsymbol{x}_1)\frac{p_t(\boldsymbol{x}|\boldsymbol{x}_1)}{p_t(\boldsymbol{x})}\right] = \int u_t(\boldsymbol{x}|\boldsymbol{x}_1)\frac{p_t(\boldsymbol{x}|\boldsymbol{x}_1)p_{\text{data}}(\boldsymbol{x})}{p_t(\boldsymbol{x})}\,\mathrm{d}\boldsymbol{x}_1.$$

Such a marginal vector field actually generates the marginal probability path.

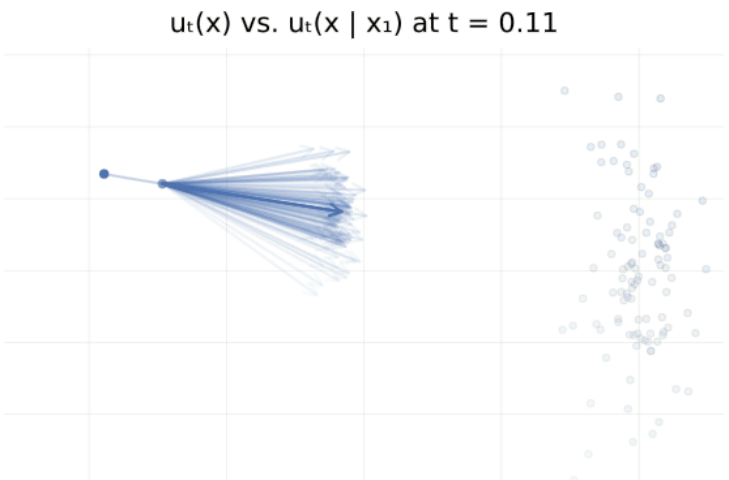

https://mlg.eng.cam.ac.uk/blog/2024/01/20/flow-matching.html

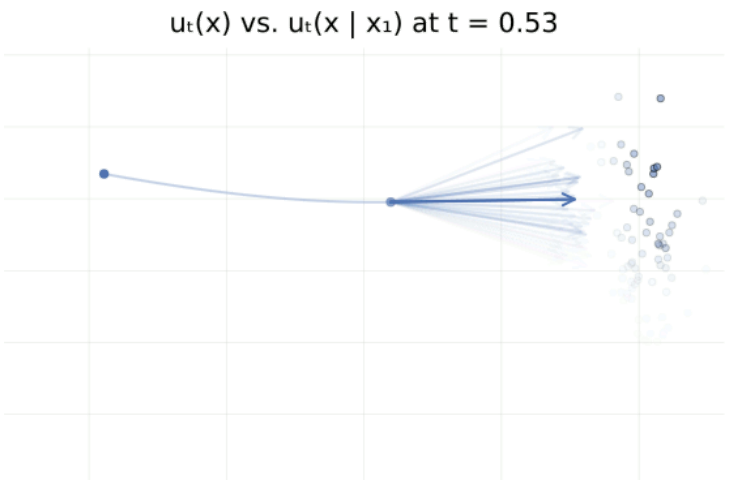

https://mlg.eng.cam.ac.uk/blog/2024/01/20/flow-matching.html

To verify that the marginal vector field generates the marginal probability path, we need to check that p_t and u_t satisfy the transport equation:

$$\begin{aligned}
\frac{d}{dt}p_t(\boldsymbol{x}) &= \mathbb{E}_{\boldsymbol{x}_1\sim p_{\text{data}}}\left[\frac{d}{dt}p_t(\boldsymbol{x}|\boldsymbol{x}_1)\right] \\
&= \mathbb{E}_{\boldsymbol{x}_1\sim p_{\text{data}}}\Big[-\operatorname{div}\big(u_t(\boldsymbol{x}|\boldsymbol{x}_t)p_t(\boldsymbol{x}|\boldsymbol{x}_1)\big)\Big] \\
&= -\operatorname{div}\Big(\mathbb{E}_{\boldsymbol{x}_1\sim p_{\text{data}}}\big[u_t(\boldsymbol{x}|\boldsymbol{x}_t)p_t(\boldsymbol{x}|\boldsymbol{x}_1)\big]\Big) \\
&= -\operatorname{div}\Big(\underbrace{\mathbb{E}_{\boldsymbol{x}_1\sim p_{\text{data}}}\big[u_t(\boldsymbol{x}|\boldsymbol{x}_t)p_t(\boldsymbol{x}|\boldsymbol{x}_1)/p_t(\boldsymbol{x})\big]}_{\text{definition of } u_t(\boldsymbol{x})}p_t(\boldsymbol{x})\Big) \\
&= -\operatorname{div}\big(u_t(\boldsymbol{x})p_t(\boldsymbol{x})\big).
\end{aligned}$$

Note that swapping a derivative and an integral requires various smoothness conditions; we assume all our objects "nice enough".

Conditional Flow Matching

Even with the definition of the marginal vector field, obtaining an unbiased estimate of the flow matching objective is still intractable (the integrals in the definition of the conditional probability path/vector field are intractable).

However, we can use the following simplified *conditional flow matching (CFM) objective*:

$$\mathcal{L}_{\text{CFM}}(\boldsymbol{\theta}) \stackrel{\text{def}}{=} \mathbb{E}_{t,\boldsymbol{x}_1\sim p_{\text{data}},\boldsymbol{x}\sim p_t(\boldsymbol{x}|\boldsymbol{x}_1)} \left\| v_t(\boldsymbol{x};\boldsymbol{\theta}) - u_t(\boldsymbol{x}|\boldsymbol{x}_1)\right\|^2.$$

This objective allows unbiased estimates, given that only the conditional variants of p_t and u_t are needed.

Importantly, while this objective $\mathcal{L}_{\text{CFM}}$ is different from the original flow matching objective $\mathcal{L}_{\text{FM}}$, it has the same gradients with respect to $\boldsymbol{\theta}$.

Conditional Flow Matching

WIP: The proof that the gradient with respect to $\boldsymbol{\theta}$ of $\mathcal{L}_{\mathrm{FM}}$ and $\mathcal{L}_{\mathrm{CFM}}$ will be added later.

Construction of the Conditional Probability Paths

We now define the conditional probability paths that we will use. We consider normal distributions with time-dependent mean $\mu_t(\boldsymbol{x}_1)$ and variance $\sigma_t^2(\boldsymbol{x}_1)$:

$$p_t(\boldsymbol{x}|\boldsymbol{x}_1) \stackrel{\text{def}}{=} \mathcal{N}\big(\boldsymbol{x}|\mu_t(\boldsymbol{x}_1), \sigma_t^2(\boldsymbol{x}_1)\boldsymbol{I}\big).$$

We require

- $\mu_0(\boldsymbol{x}_1) = 0$ and $\sigma_0^2(\boldsymbol{x}_1) = 1$ so that $p_0(\boldsymbol{x}|\boldsymbol{x}_1) = p_0(\boldsymbol{x})$, and
- $\mu_t(\boldsymbol{x}_1) = \boldsymbol{x}_1$ and $\sigma_1^2(\boldsymbol{x}_1) = \sigma_{\text{min}}^2$ so that $p_1(\boldsymbol{x}|\boldsymbol{x}_1)$ is concentrated around $\boldsymbol{x}_1$.

While there are infinitely many vector fields generating these probability paths, we use the simplest one, corresponding to the flow (dependent on $\boldsymbol{x}_1$)

$$\varphi_t(\boldsymbol{x}) = \sigma_t(\boldsymbol{x}_1)\boldsymbol{x} + \mu_t(\boldsymbol{x}_1),$$

which is an affine transformation mapping standard normal distribution to a normal distribution with mean $\mu_t(\boldsymbol{x}_1)$ and variance $\sigma_t^2(\boldsymbol{x}_1)$.

Construction of the Conditional Vector Field

We now derive the conditional vector field $u_t(\boldsymbol{x}|\boldsymbol{x}_1)$ so that its flow is the defined

$$\varphi_t(\boldsymbol{x}) = \sigma_t(\boldsymbol{x}_1)\boldsymbol{x} + \mu_t(\boldsymbol{x}_1).$$

Recalling the flow ODE $\frac{d}{dt}\varphi_t(\boldsymbol{x}) = u_t(\varphi_t(\boldsymbol{x}))$, it could be used to defined u_t, but unfortunately for $\varphi_t(\boldsymbol{x})$, not for arbitrary $\boldsymbol{x}$.

However, the affine map φ_t has an analytical inverse (assuming $\sigma_t(\boldsymbol{x}_1) > 0$)

$$\varphi_t^{-1}(\boldsymbol{z}) = \frac{\boldsymbol{z} - \mu_t(\boldsymbol{x}_1)}{\sigma_t(\boldsymbol{x}_1)}.$$

Therefore, when we consider $\boldsymbol{z} = \varphi_t(\boldsymbol{x})$, we get $u_t(\boldsymbol{z}|\boldsymbol{x}_1) = \varphi_t'(\varphi_t^{-1}(\boldsymbol{z}))$.

Using the derivative $\varphi_t'(\boldsymbol{x}|\boldsymbol{x}_1) = \sigma_t'(\boldsymbol{x}_1)\boldsymbol{x} + \mu_t'(\boldsymbol{x}_1)$, we obtain that

$$u_t(\boldsymbol{z}|\boldsymbol{x}_1) = \frac{\sigma_t'(\boldsymbol{x}_1)}{\sigma_t(\boldsymbol{x}_1)}\big(\boldsymbol{z} - \mu_t(\boldsymbol{x}_1)\big) + \mu_t'(\boldsymbol{x}_1).$$

Construction of the Conditional Vector Field

The authors propose to use conditional paths with mean and variance changing linearly in t:

$$\mu_t(\boldsymbol{x}_1) \stackrel{\text{def}}{=} t\boldsymbol{x}_1, \quad \sigma_t(\boldsymbol{x}_1) \stackrel{\text{def}}{=} 1 - (1 - \sigma_{\min})t.$$

Therefore, the corresponding flow and vector field are

$$\varphi_t(\boldsymbol{x}) = (1 - (1 - \sigma_{\min})t)\boldsymbol{x} + t\boldsymbol{x}_1, \qquad \textit{such a flow is called Optimal Transport}$$

$$u_t(\boldsymbol{x}|\boldsymbol{x}_1) = \frac{-(1 - \sigma_{\min})}{1 - (1 - \sigma_{\min})t}\big(\boldsymbol{x} - t\boldsymbol{x}_1\big) + \boldsymbol{x}_1 = \frac{\boldsymbol{x}_1 - (1 - \sigma_{\min})\boldsymbol{x}}{1 - (1 - \sigma_{\min})t}.$$

Finally, recalling the general form $\mathcal{L}_{\text{CFM}}(\boldsymbol{\theta}) \stackrel{\text{def}}{=} \mathbb{E}_{t,\boldsymbol{x}_1\sim p_{\text{data}},\boldsymbol{x}\sim p_t(\boldsymbol{x}|\boldsymbol{x}_1)} \big\|v_t(\boldsymbol{x};\boldsymbol{\theta}) - u_t(\boldsymbol{x}|\boldsymbol{x}_1)\big\|^2$, for our specific case of OT flow we obtain

$$\mathcal{L}_{\text{CFM}}(\boldsymbol{\theta}) \stackrel{\text{def}}{=} \mathbb{E}_{t,\boldsymbol{x}_1\sim p_{\text{data}},\boldsymbol{x}_0\sim p_0} \Big\|v_t\big(\varphi_t(\boldsymbol{x}_0);\boldsymbol{\theta}\big) - \big(\boldsymbol{x}_1 - (1 - \sigma_{\min})\boldsymbol{x}_0\big)\Big\|^2.$$

Conditional Probability Paths and Marginal Probability Paths

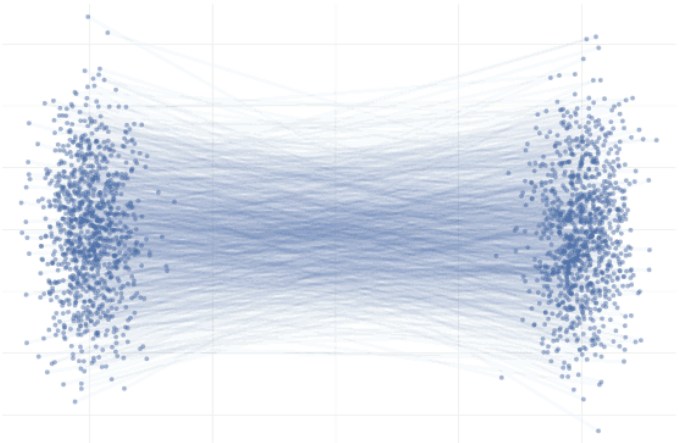

https://mlg.eng.cam.ac.uk/blog/2024/01/20/flow-matching.html

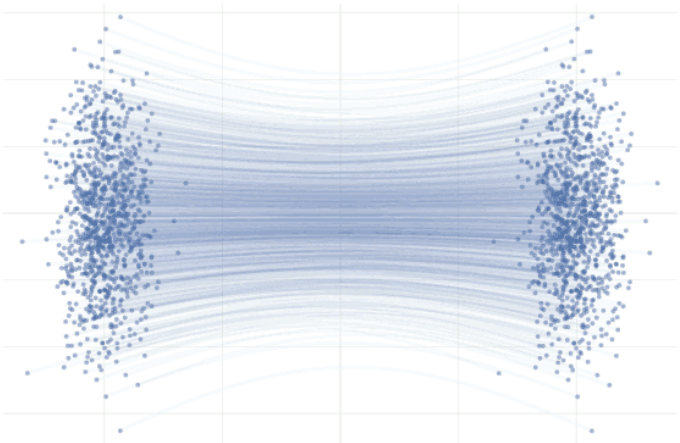

https://mlg.eng.cam.ac.uk/blog/2024/01/20/flow-matching.html

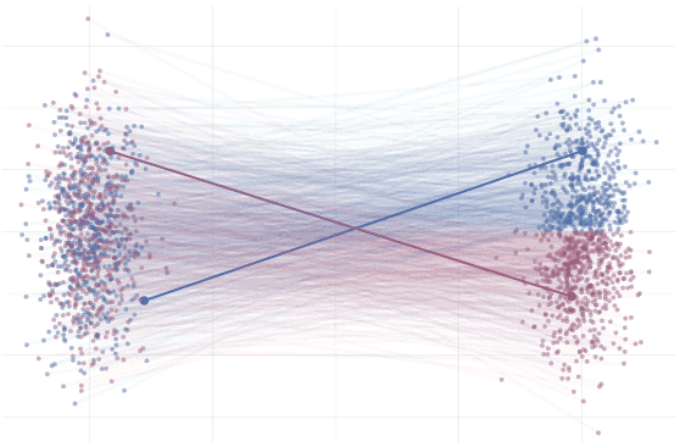

https://mlg.eng.cam.ac.uk/blog/2024/01/20/flow-matching.html

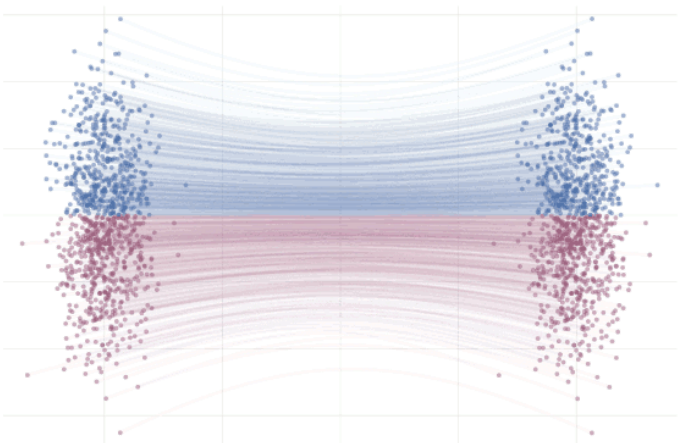

https://mlg.eng.cam.ac.uk/blog/2024/01/20/flow-matching.html

Conditional Probability Paths and Marginal Probability Paths

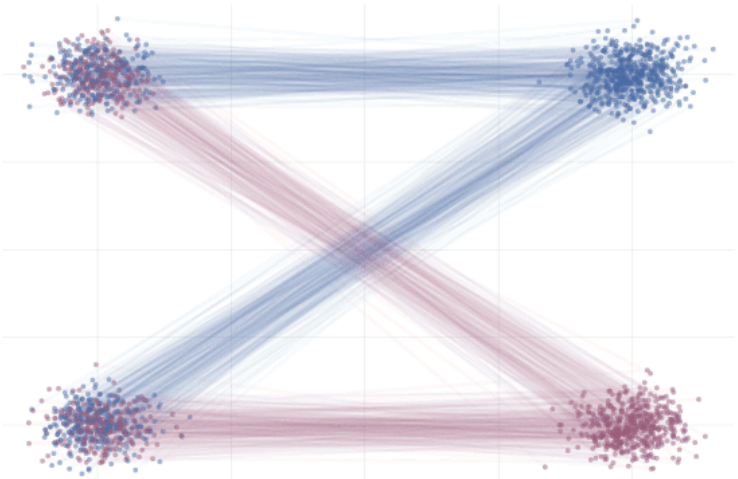

https://mlg.eng.cam.ac.uk/blog/2024/01/20/flow-matching.html

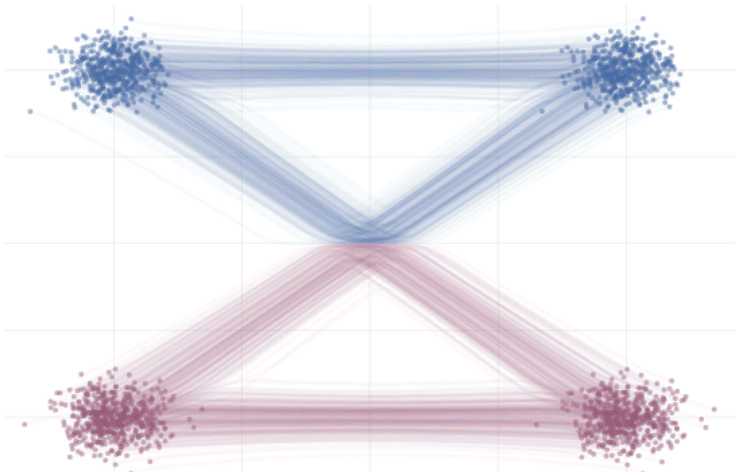

https://mlg.eng.cam.ac.uk/blog/2024/01/20/flow-matching.html

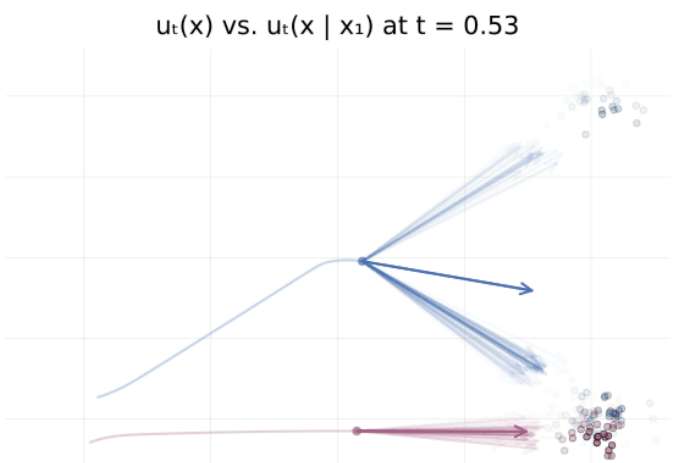

https://mlg.eng.cam.ac.uk/blog/2024/01/20/flow-matching.html

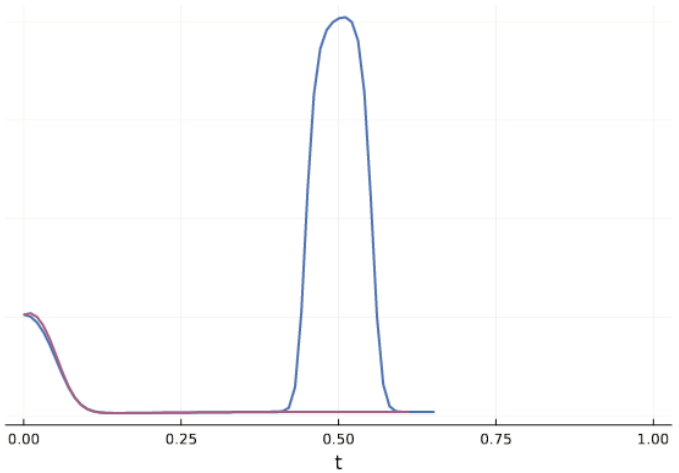

https://mlg.eng.cam.ac.uk/blog/2024/01/20/flow-matching.html

Conditional Flow Matching Algorithm

Let $v_t(\boldsymbol{x}; \boldsymbol{\theta})$ be a UNet-like neural network model predicting the vector field.

Training

During training, we minimize CFM objective by SGD/Adam:

$$\mathcal{L}_{\mathrm{CFM}}(\boldsymbol{\theta}) \stackrel{\mathrm{def}}{=} \mathbb{E}_{t, \boldsymbol{x}_1 \sim p_{\mathrm{data}}, \boldsymbol{x}_0 \sim p_0} \left\| v_t\big(\varphi_t(\boldsymbol{x}_0); \boldsymbol{\theta}\big) - \big(\boldsymbol{x}_1 - (1 - \sigma_{\min})\boldsymbol{x}_0\big) \right\|^2.$$

Specifically, we generate batches of training data $\boldsymbol{X} \sim p_{\mathrm{data}}$ as usual, for each batch example we also generate $t \sim U[0, 1]$ and $\boldsymbol{x}_0 \sim \mathcal{N}(\boldsymbol{0}, \boldsymbol{I})$, and we minimize the mean squared error

$$\left\| v_t\big(\varphi_t(\boldsymbol{x}_0); \boldsymbol{\theta}\big) - \big(\boldsymbol{x}_1 - (1 - \sigma_{\min})\boldsymbol{x}_0\big) \right\|^2.$$

Sampling

In order to generate an image, we start by sampling $\mathbf{x}_0 \sim p_0$, and then perform numerical integration by the Euler method using T steps by

$$\boldsymbol{x}_{t+1/T} \leftarrow \boldsymbol{x}_t + \tfrac{1}{T} v_t(\boldsymbol{x}_t; \boldsymbol{\theta}).$$

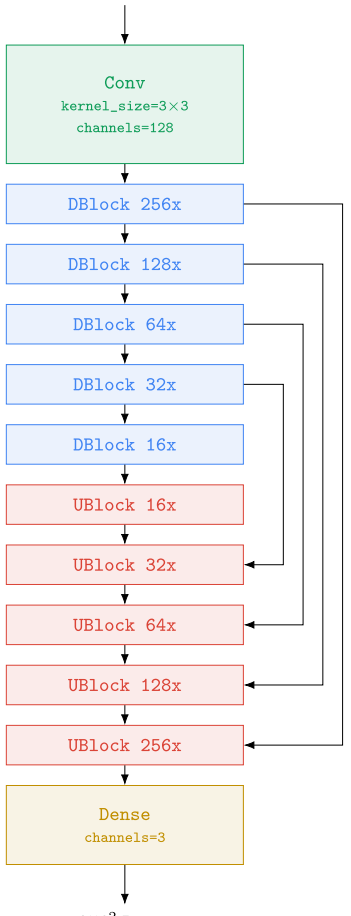

Figure A.30 of "Photorealistic Text-to-Image Diffusion Models with Deep Language Understanding", https://arxiv.org/abs/2205.11487

Further Reading About Flow Matching

- An introduction to Flow Matching https://mlg.eng.cam.ac.uk/blog/2024/01/20/flow-matching.html#fn:mini-batch-ot-deterministic-vs-stochastic
- A Visual Dive into Conditional Flow Matching https://dl.heeere.com/conditional-flow-matching/blog/conditional-flow-matching/
- Diffusion Meets Flow Matching: Two Sides of the Same Coin https://diffusionflow.github.io/

Architectures of Diffusion Models, Suitable Also for FM

Vector field $v_t(\boldsymbol{x}; \boldsymbol{\theta})$ can be predicted by UNet architecture with pre-activated ResNet blocks.

- The current continuous time step is represented using the Transformer sinusoidal embeddings and added "in the middle" of every residual block (after the first convolution).
- Additionally, on several lower-resolution levels, a self-attention block (an adaptation of the Transformer self-attention, which considers the 2D grid of features as a sequence of feature vectors) is commonly used. Because the complexity is asymptotically the image width to the power of four, only the lower-resolution levels are used for this self-attention.

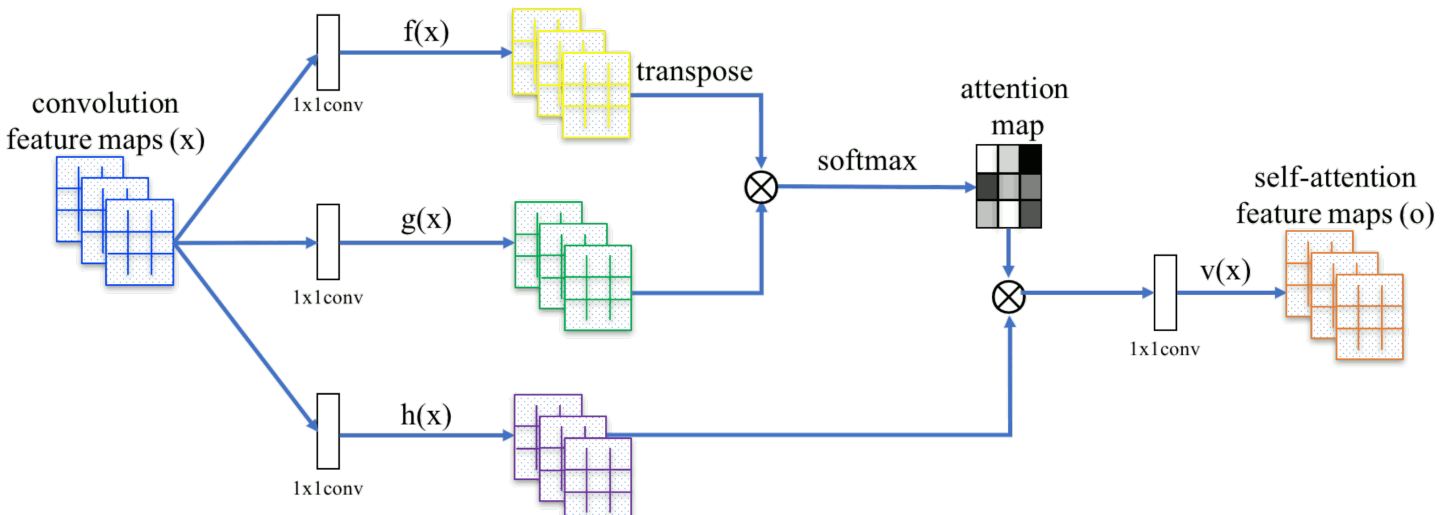

Figure 2 of "Self-Attention Generative Adversarial Networks", https://arxiv.org/abs/1805.08318

Diffusion Models Architecture – ImaGen

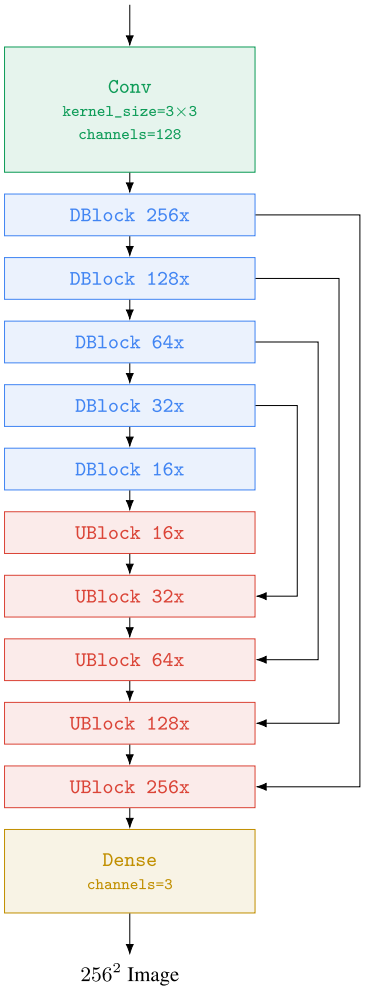

Figure A.30 of "Photorealistic Text-to-Image Diffusion Models with Deep Language Understanding", https://arxiv.org/abs/2205.11487

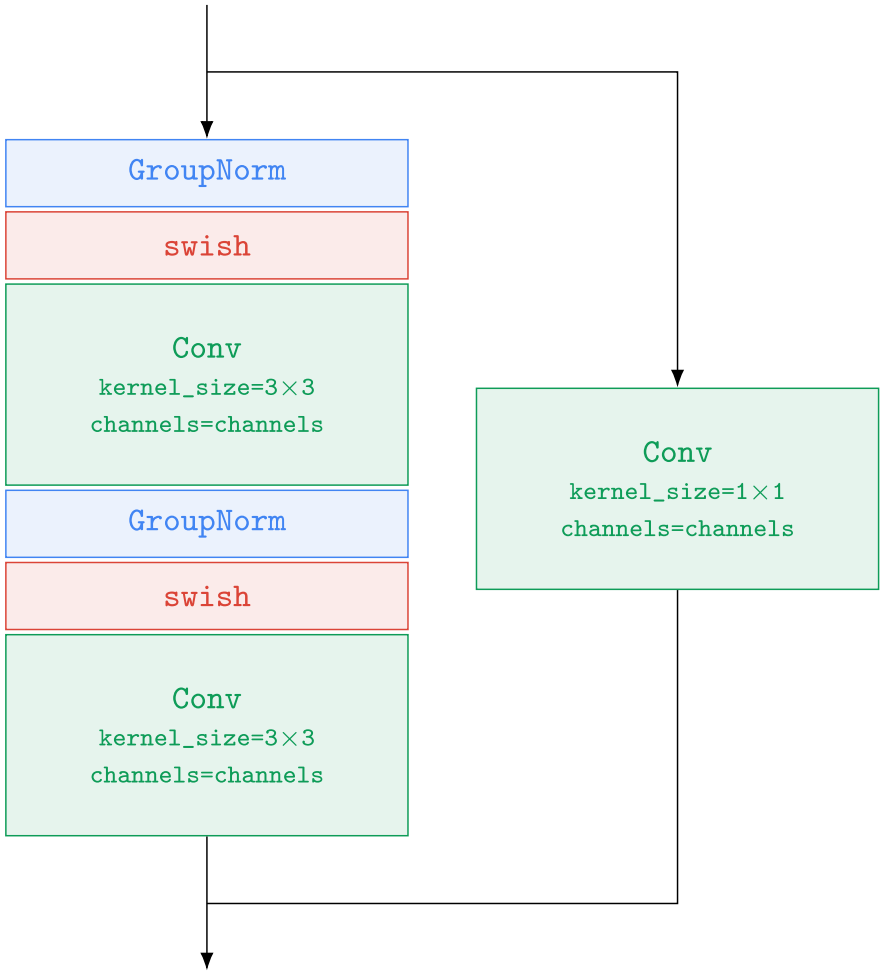

Figure A.27 of "Photorealistic Text-to-Image Diffusion Models with Deep Language Understanding", https://arxiv.org/abs/2205.11487

Diffusion Models Architecture – ImaGen

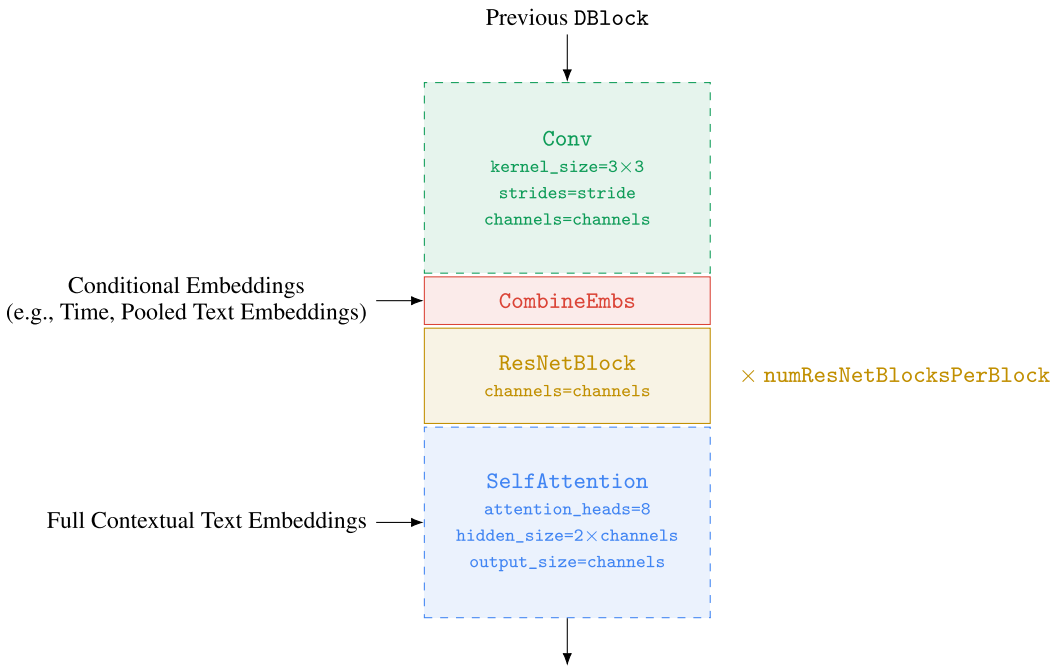

Figure A.28 of "Photorealistic Text-to-Image Diffusion Models with Deep Language Understanding", https://arxiv.org/abs/2205.11487

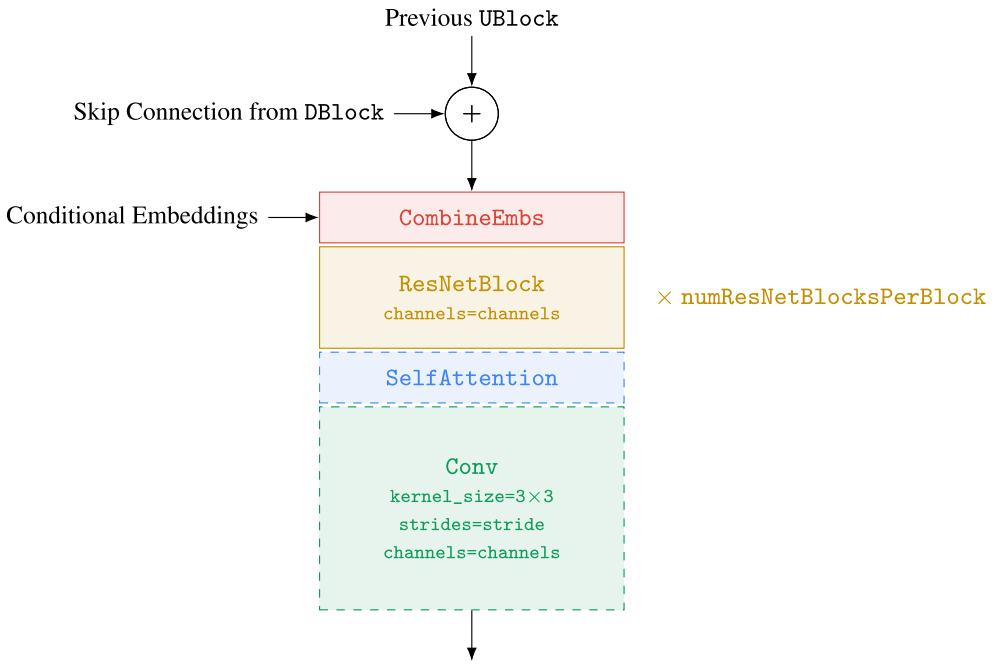

Figure A.29 of "Photorealistic Text-to-Image Diffusion Models with Deep Language Understanding", https://arxiv.org/abs/2205.11487

There are of course many possible variants; furthermore, Visual Transformer can be used instead of the UNet architecture.

Conditional Models, Classifier-Free Guidance

In many cases we want the generative model to be conditional. We have already seen how to condition it on the current time step. Additionally, we might consider also conditioning on

- an image (e.g., for super-resolution): the image is then resized and concatenated with the input noised image (and optionally in other places, like after every resolution change);
- a text: the usual approach is to encode the text using some pre-trained encoder, and then to introduce an "image-text" attention layer (usually after the self-attention layers).

To make the effect of conditioning stronger during sampling, we might also employ *classifier-free guidance*:

- During training, we sometimes train $v_t(\boldsymbol{x}, y; \boldsymbol{\theta})$ with the conditioning y, and sometimes we train $v_t(\boldsymbol{x}, \varnothing; \boldsymbol{\theta})$ without the conditioning.
- During sampling, we pronounce the effect of the conditioning by taking the unconditioned vector field and adding the difference between conditioned and unconditioned vector field *weighted by the weight* w (values like $w = 5$ or $w = 7.5$ are mentioned in papers):

$$v_t(\boldsymbol{x}, \varnothing; \boldsymbol{\theta}) + w\big(v_t(\boldsymbol{x}, y; \boldsymbol{\theta}) - v_t(\boldsymbol{x}_t, \varnothing; \boldsymbol{\theta})\big).$$

Samples from Model Trained on the Practicals

Samples from Conditional Model Trained on the Practicals

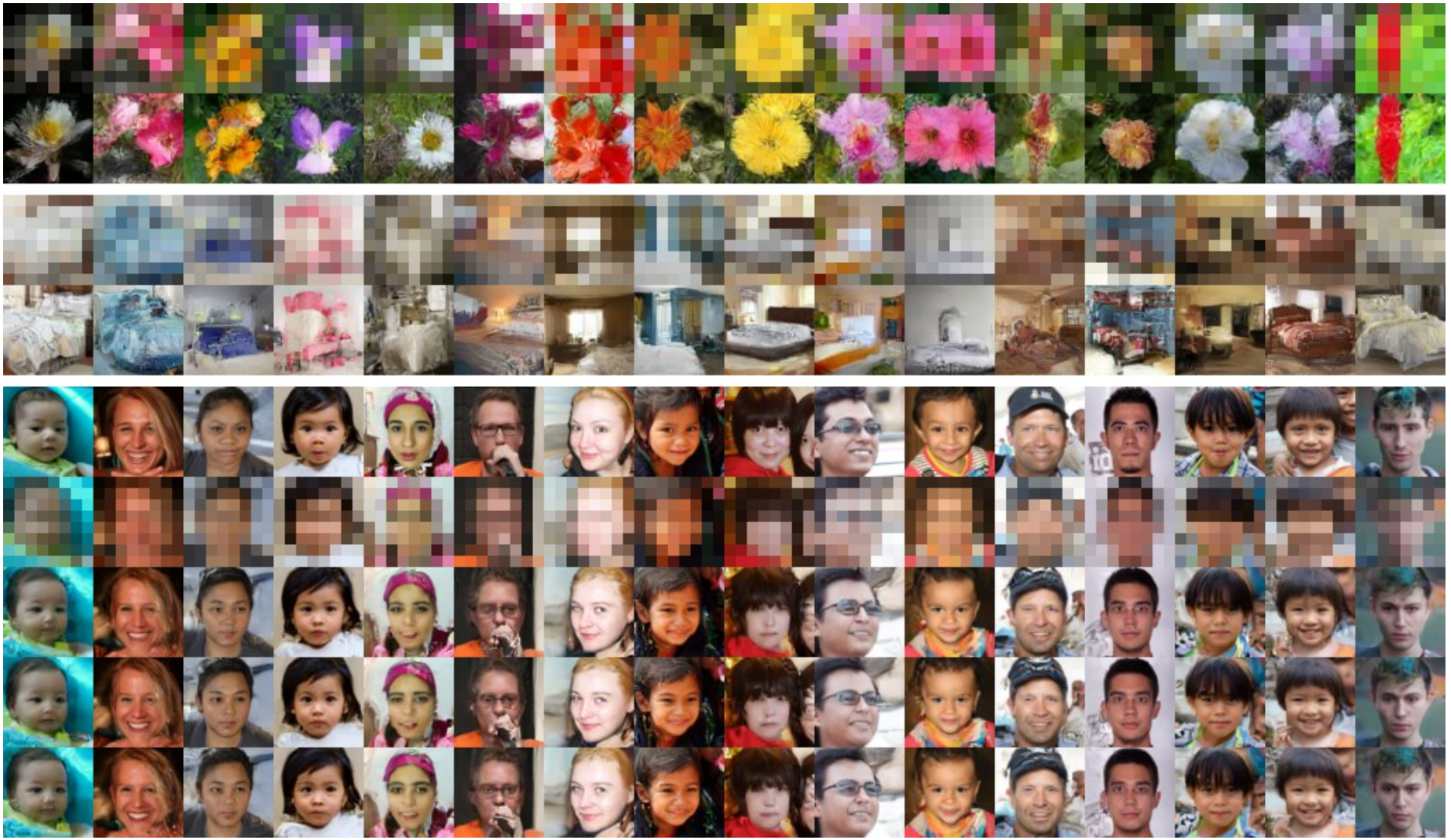

Diffusion Models

Diffusion Models: Overview of the Overall Process

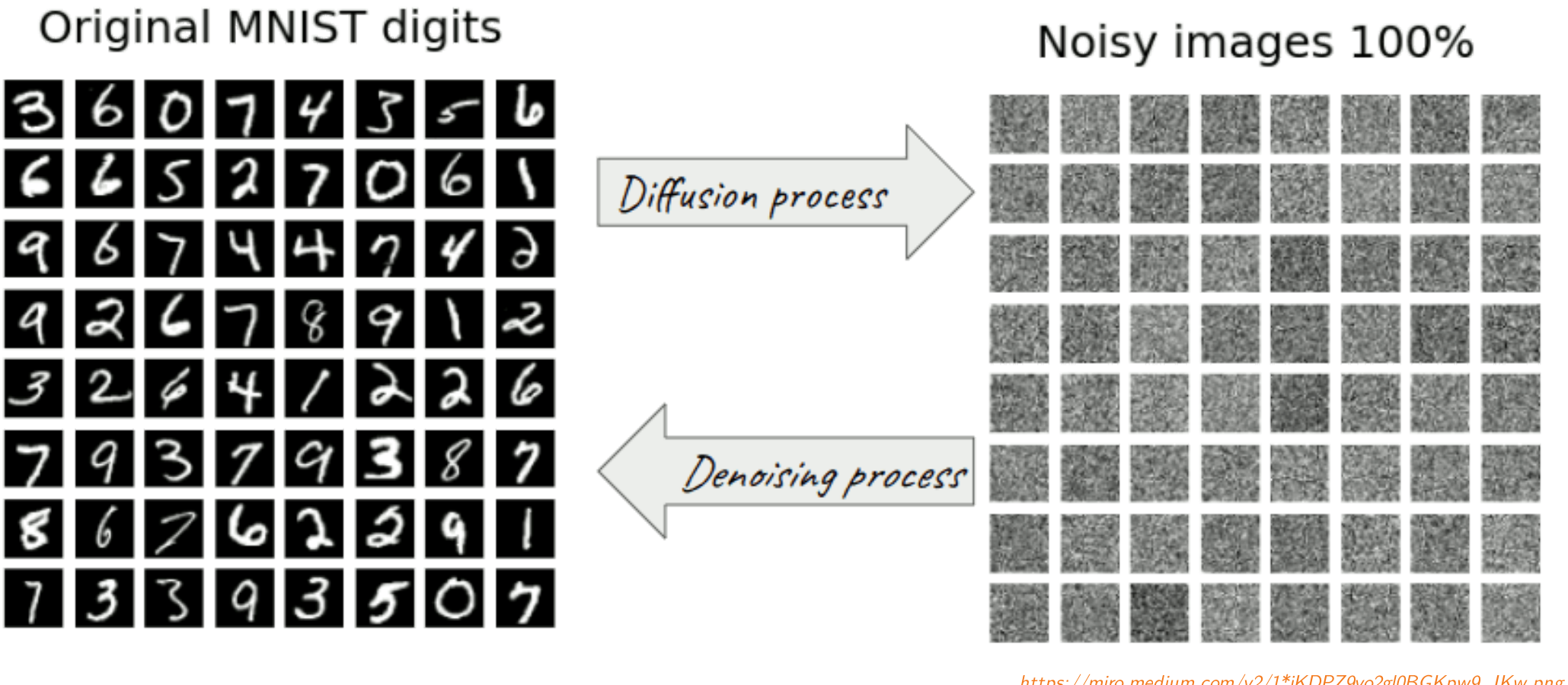

https://miro.medium.com/v2/1*jKDPZ9vo2gl0BGKpw9_IKw.png

Diffusion Models – Diffusion Process, Reverse Process

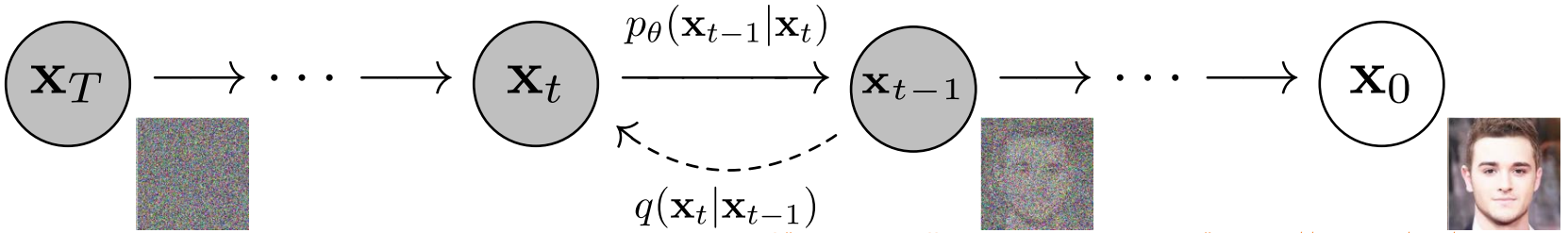

Figure 2 of "Denoising Diffusion Probabilistic Models", https://arxiv.org/abs/2006.11239

Given a data point $\mathbf{x}_0$ from a real data distribution $q(\mathbf{x})$, we define a T-step *diffusion process* (or the *forward process*) which gradually adds Gaussian noise to the input image:

$$q(\mathbf{x}_{1:T}|\mathbf{x}_0) = \prod_{t=1}^{T} q(\mathbf{x}_t|\mathbf{x}_{t-1}).$$

Our goal is to reverse the forward process $q(\mathbf{x}_t|\mathbf{x}_{t-1})$, and generate an image by starting with $\mathbf{x}_T \sim \mathcal{N}(\mathbf{0}, \boldsymbol{I})$, and then performing the forward process in reverse. We therefore learn a model $p_{\boldsymbol{\theta}}(\mathbf{x}_{t-1}|\mathbf{x}_t)$ to approximate the reverse of $q(\mathbf{x}_t|\mathbf{x}_{t-1})$, and obtain a *reverse process*:

$$p_{\boldsymbol{\theta}}(\mathbf{x}_{0:T}) = p(\mathbf{x}_T) \prod_{t=1}^{T} p_{\boldsymbol{\theta}}(\mathbf{x}_{t-1}|\mathbf{x}_t).$$

Diffusion Models – Model Overview

The $p_{\boldsymbol{\theta}}(\mathbf{x}_{t-1}|\mathbf{x}_t)$ is commonly modelled using a UNet architecture with skip connections.

Training

During training, we randomly sample a time step t, and perform an update of the parameters $\boldsymbol{\theta}$ in order for $p_{\boldsymbol{\theta}}(\mathbf{x}_{t-1}|\mathbf{x}_t)$ to better approximate the reverse of $q(\mathbf{x}_t|\mathbf{x}_{t-1})$.

Sampling

In order to sample an image, we start by sampling $\mathbf{x}_T \sim \mathcal{N}(\mathbf{0}, \boldsymbol{I})$, and then perform T steps of the reverse process by sampling $\mathbf{x}_{t-1} \sim p_{\boldsymbol{\theta}}(\mathbf{x}_{t-1}|\mathbf{x}_t)$ for t from T down to 1.

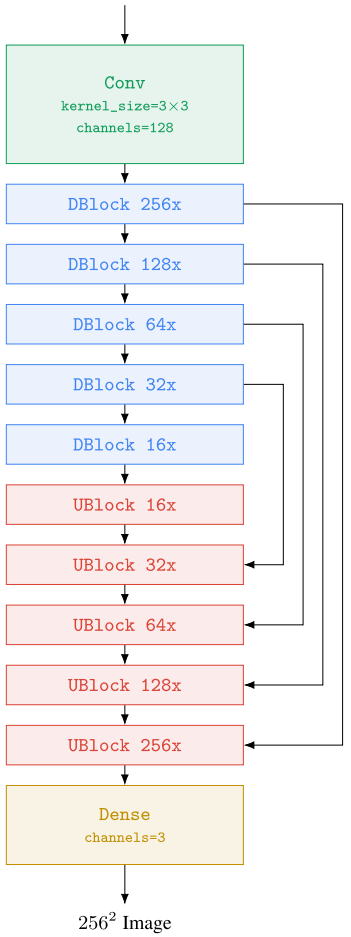

Figure A.30 of "Photorealistic Text-to-Image Diffusion Models with Deep Language Understanding", https://arxiv.org/abs/2205.11487

Normal Distribution Reminder

Normal (or Gaussian) distribution is a continuous distribution parametrized by a mean μ and variance σ^2:

$$\mathcal{N}(x; \mu, \sigma^2) = \sqrt{\frac{1}{2\pi\sigma^2}} \exp\left(-\frac{(x-\mu)^2}{2\sigma^2}\right)$$

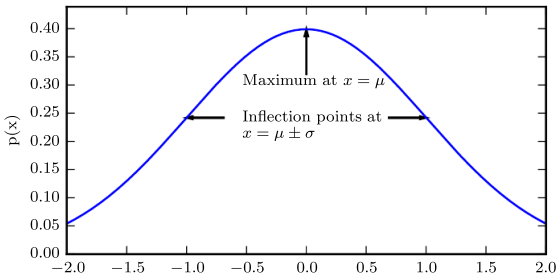

Figure 3.1 of "Deep Learning" book, https://www.deeplearningbook.org

For a D-dimensional vector $\boldsymbol{x}$, the multivariate Gaussian distribution takes the form

$$\mathcal{N}(\boldsymbol{x}; \boldsymbol{\mu}, \boldsymbol{\Sigma}) \stackrel{\text{def}}{=} \frac{1}{\sqrt{(2\pi)^D |\boldsymbol{\Sigma}|}} \exp\left(-\frac{1}{2}(\boldsymbol{x}-\boldsymbol{\mu})^T \boldsymbol{\Sigma}^{-1} (\boldsymbol{x}-\boldsymbol{\mu})\right).$$

The biggest difference compared to the single-dimensional case is the *covariance matrix* $\boldsymbol{\Sigma}$, which is (in the non-degenerate case, which is the only one considered here) a *symmetric positive-definite matrix* of size $D \times D$.

However, in this lecture we will only consider *isotropic* distribution, where $\boldsymbol{\Sigma} = \sigma^2 \boldsymbol{I}$:

$$\mathcal{N}(\boldsymbol{x}; \boldsymbol{\mu}, \sigma^2 \boldsymbol{I}) = \prod_i \mathcal{N}(x_i; \mu_i, \sigma^2).$$

Normal Distribution Reminder

- A normally-distributed random variable $\mathbf{x} \sim \mathcal{N}(\boldsymbol{\mu}, \sigma^2 \boldsymbol{I})$ can be written using the reparametrization trick also as

$$\mathbf{x} = \boldsymbol{\mu} + \sigma \mathbf{e}, \text{ where } \mathbf{e} \sim \mathcal{N}(\mathbf{0}, \boldsymbol{I}).$$

- The sum of two independent normally-distributed random variables $\mathbf{x}_1 \sim \mathcal{N}(\boldsymbol{\mu}_1, \sigma_1^2 \boldsymbol{I})$ and $\mathbf{x}_2 \sim \mathcal{N}(\boldsymbol{\mu}_2, \sigma_2^2 \boldsymbol{I})$ has normal distribution $\mathcal{N}\big(\boldsymbol{\mu}_1 + \boldsymbol{\mu}_2, (\sigma_1^2 + \sigma_2^2)\boldsymbol{I}\big)$.

  Therefore, if we have two standard normal random variables $\mathbf{e}_1, \mathbf{e}_2 \sim \mathcal{N}(\mathbf{0}, \boldsymbol{I})$, then

$$\sigma_1 \mathbf{e}_1 + \sigma_2 \mathbf{e}_2 = \sqrt{\sigma_1^2 + \sigma_2^2}\,\mathbf{e}$$

  for a standard normal random variable $\mathbf{e} \sim \mathcal{N}(\mathbf{0}, \boldsymbol{I})$.

DDPM – The Forward Process

We now describe *Denoising Diffusion Probabilistic Models (DDPM)*.

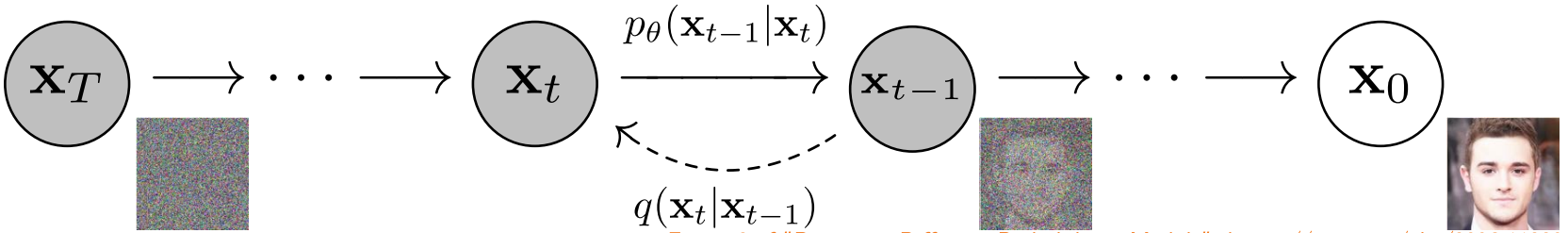

Figure 2 of "Denoising Diffusion Probabilistic Models", https://arxiv.org/abs/2006.11239

Given a data point $\mathbf{x}_0$ from a real data distribution $q(\mathbf{x})$, we define a T-step *diffusion process* (or the *forward process*) which gradually adds Gaussian noise according to some variance schedule $\beta_1, \ldots, \beta_T$:

$$q(\mathbf{x}_{1:T}|\mathbf{x}_0) = \prod_{t=1}^{T} q(\mathbf{x}_t|\mathbf{x}_{t-1}),$$

$$q(\mathbf{x}_t|\mathbf{x}_{t-1}) = \mathcal{N}(\mathbf{x}_t; \sqrt{1-\beta_t}\mathbf{x}_{t-1}, \beta_t \boldsymbol{I}),$$

$$= \sqrt{1-\beta_t}\mathbf{x}_{t-1} + \sqrt{\beta_t}\mathbf{e} \text{ for } \mathbf{e} \sim \mathcal{N}(\mathbf{0}, \boldsymbol{I}).$$

More noise gets gradually added to the original image $\mathbf{x}_0$, converging to pure Gaussian noise.

DDPM – The Forward Process

Let $\alpha_t = 1 - \beta_t$ and $\bar{\alpha}_t = \prod_{i=1}^{t} \alpha_i$. Then we have

$$\begin{aligned}
\mathbf{x}_t &= \sqrt{\alpha_t}\mathbf{x}_{t-1} + \sqrt{1-\alpha_t}\mathbf{e}_t \\
&= \sqrt{\alpha_t}\left(\sqrt{\alpha_{t-1}}\mathbf{x}_{t-2} + \sqrt{1-\alpha_{t-1}}\mathbf{e}_{t-1}\right) + \sqrt{1-\alpha_t}\mathbf{e}_t \\
&= \sqrt{\alpha_t\alpha_{t-1}}\mathbf{x}_{t-2} + \sqrt{\alpha_t(1-\alpha_{t-1}) + (1-\alpha_t)}\bar{\mathbf{e}}_{t-1} \\
&= \sqrt{\alpha_t\alpha_{t-1}}\mathbf{x}_{t-2} + \sqrt{1-\alpha_t\alpha_{t-1}}\bar{\mathbf{e}}_{t-1} \\
&= \sqrt{\alpha_t\alpha_{t-1}\alpha_{t-2}}\mathbf{x}_{t-3} + \sqrt{1-\alpha_t\alpha_{t-1}\alpha_{t-2}}\bar{\mathbf{e}}_{t-2} \\
&= \dots \\
&= \sqrt{\bar{\alpha}_t}\mathbf{x}_0 + \sqrt{1-\bar{\alpha}_t}\bar{\mathbf{e}}_0
\end{aligned}$$

for standard normal random variables $\mathbf{e}_i$ and $\bar{\mathbf{e}}_i$.

In other words, we have shown that $q(\mathbf{x}_t|\mathbf{x}_0) = \mathcal{N}\left(\sqrt{\bar{\alpha}_t}\mathbf{x}_0, (1-\bar{\alpha}_t)\boldsymbol{I}\right)$.

Therefore, if $\bar{\alpha}_t \to 0$ as $t \to \infty$, the $\mathbf{x}_t$ converges to $\mathcal{N}(\mathbf{0}, \boldsymbol{I})$ as $t \to \infty$.

DDPM – The Forward Process

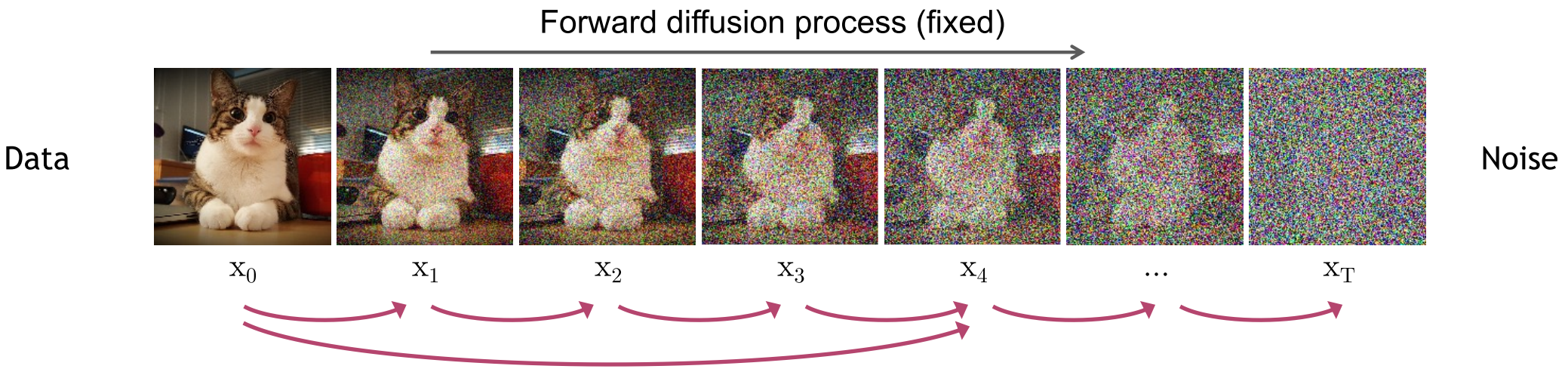

CVPR 2022 tutorial https://cvpr2022-tutorial-diffusion-models.github.io/

DDPM – Noise Schedule

Originally, linearly increasing sequence of noise variations $\beta_1 = 0.0001, \ldots, \beta_T = 0.04$ was used.

However, the resulting sequence $\bar{\alpha}_t$ was not ideal (nearly the whole second half of the diffusion process was mostly just random noise), so later a cosine schedule was proposed:

$$\bar{\alpha}_t = \frac{1}{2}\Big(\cos(t/T \cdot \pi) + 1\Big).$$

In practice, we want to avoid both the values of 0 and 1, and keep α_t in $[\varepsilon, 1-\varepsilon]$ range.

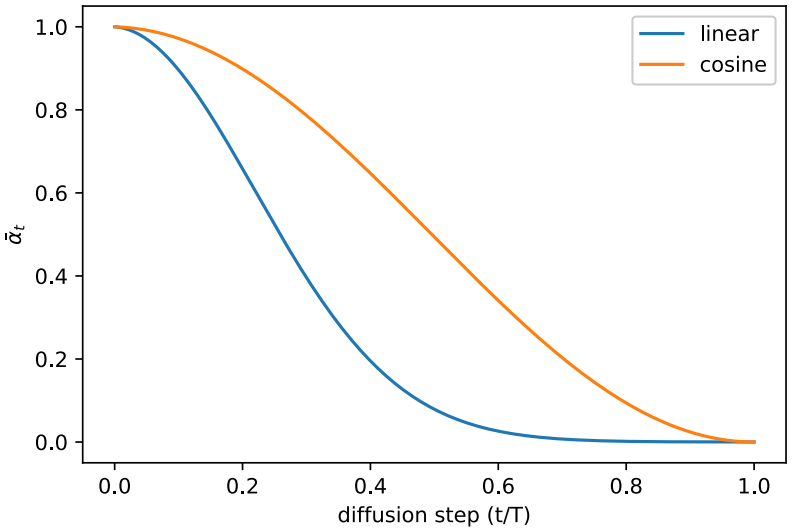

Figure 5. $\bar{\alpha}_t$ throughout diffusion in the linear schedule and our proposed cosine schedule.

Figure 5 of "Improved Denoising Diffusion Probabilistic Models", https://arxiv.org/abs/2102.09672

DDPM – Noise Schedule

We assume the images $\mathbf{x}_0$ have zero mean and unit variance (we normalize them to achieve that). Then every

$$q(\mathbf{x}_t|\mathbf{x}_0) = \sqrt{\bar{\alpha}_t}\mathbf{x}_0 + \sqrt{1-\bar{\alpha}_t}\mathbf{e}$$

has also zero mean and unit variance.

The $\sqrt{\bar{\alpha}_t}$ and $\sqrt{1-\bar{\alpha}_t}$ can be considered as the *signal rate* and the *noise rate*.

Because $\sqrt{\bar{\alpha}_t}^2 + \sqrt{1-\bar{\alpha}_t}^2 = 1$, the signal rate and the noise rate form a circular arc. The proposed cosine schedule

$$\sqrt{\bar{\alpha}_t} = \cos(t/T \cdot \pi/2),$$
$$\sqrt{1-\bar{\alpha}_t} = \sin(t/T \cdot \pi/2),$$

corresponds to an uniform movement on this arc.

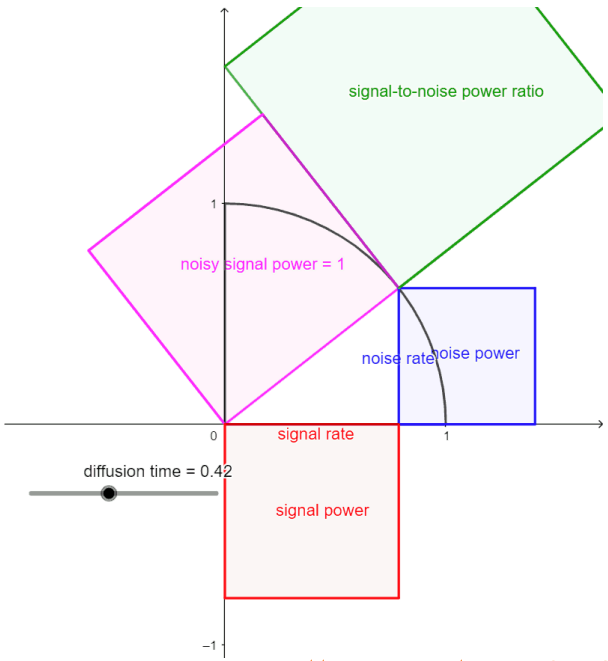

https://i.imgur.com/JW9W0fA.gif

DDPM – The Reverse Process

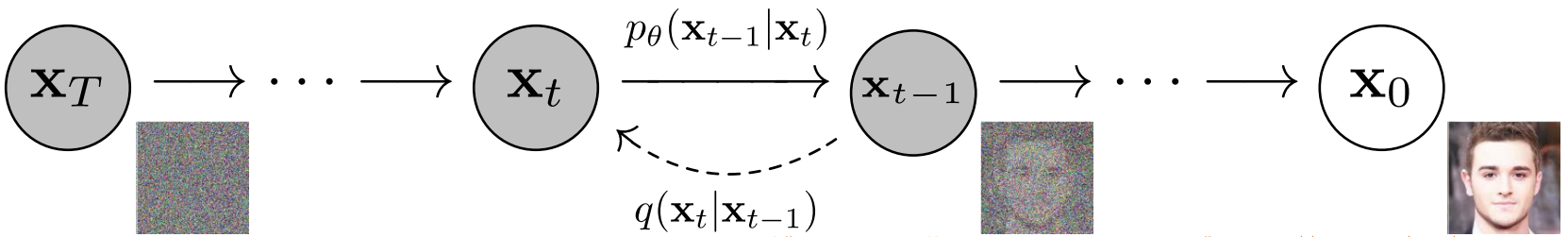

Figure 2 of "Denoising Diffusion Probabilistic Models", https://arxiv.org/abs/2006.11239

In order to be able to generate images, we therefore learn a model $p_{\boldsymbol{\theta}}(\mathbf{x}_{t-1}|\mathbf{x}_t)$ to approximate the reverse of $q(\mathbf{x}_t|\mathbf{x}_{t-1})$.

When β_t is small, this reverse is nearly Gaussian, so we represent $p_{\boldsymbol{\theta}}$ as

$$p_{\boldsymbol{\theta}}(\mathbf{x}_{t-1}|\mathbf{x}_t) = \mathcal{N}\left(\mathbf{x}_{t-1}; \boldsymbol{\mu}_{\boldsymbol{\theta}}(\mathbf{x}_t, t), \sigma_t^2 \boldsymbol{I}\right)$$

for some fixed sequence of $\sigma_1, \ldots, \sigma_T$.

The whole reverse process is then

$$p_{\boldsymbol{\theta}}(\mathbf{x}_{0:T}) = p(\mathbf{x}_T) \prod_{t=1}^{T} p_{\boldsymbol{\theta}}(\mathbf{x}_{t-1}|\mathbf{x}_t).$$

DDPM – Loss

We now want to derive the loss. First note that the reverse of $q(\mathbf{x}_t|\mathbf{x}_{t-1})$ is actually tractable when conditioning on $\mathbf{x}_0$:

$$q(\mathbf{x}_{t-1}|\mathbf{x}_t, \mathbf{x}_0) = \mathcal{N}\left(\mathbf{x}_{t-1}; \tilde{\boldsymbol{\mu}}_t(\mathbf{x}_t, \mathbf{x}_0), \tilde{\beta}_t \boldsymbol{I}\right),$$

$$\tilde{\boldsymbol{\mu}}_t(\mathbf{x}_t, \mathbf{x}_0) = \frac{\sqrt{\bar{\alpha}_{t-1}}\beta_t}{1-\bar{\alpha}_t}\mathbf{x}_0 + \frac{\sqrt{\alpha_t}(1-\bar{\alpha}_{t-1})}{1-\bar{\alpha}_t}\mathbf{x}_t,$$

$$\tilde{\beta}_t = \frac{1-\bar{\alpha}_{t-1}}{1-\bar{\alpha}_t}\beta_t.$$

We present the proof on the next slide for completeness.

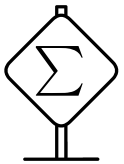

Starting with the Bayes' rule, we get

$$q(\mathbf{x}_{t-1}|\mathbf{x}_t,\mathbf{x}_0) = q(\mathbf{x}_t|\mathbf{x}_{t-1},\mathbf{x}_0)\frac{q(\mathbf{x}_{t-1}|\mathbf{x}_0)}{q(\mathbf{x}_t|\mathbf{x}_0)}$$

$$\propto \exp\Big(-\frac{1}{2}\Big(\frac{(\mathbf{x}_t-\sqrt{\alpha_t}\mathbf{x}_{t-1})^2}{\beta_t}+\frac{(\mathbf{x}_{t-1}-\sqrt{\bar\alpha_{t-1}}\mathbf{x}_0)^2}{1-\bar\alpha_{t-1}}-\frac{(\mathbf{x}_t-\sqrt{\bar\alpha_t}\mathbf{x}_0)^2}{1-\bar\alpha_t}\Big)\Big)$$

$$= \exp\Big(-\frac{1}{2}\Big(\frac{\mathbf{x}_t^2-2\sqrt{\alpha_t}\mathbf{x}_t\mathbf{x}_{t-1}+\alpha_t\mathbf{x}_{t-1}^2}{\beta_t}+\frac{\mathbf{x}_{t-1}^2-2\sqrt{\bar\alpha_{t-1}}\mathbf{x}_{t-1}\mathbf{x}_0+\bar\alpha_{t-1}\mathbf{x}_0^2}{1-\bar\alpha_{t-1}}+\dots\Big)\Big)$$

$$= \exp\Big(-\frac{1}{2}\Big(\Big(\frac{\alpha_t}{\beta_t}+\frac{1}{1-\bar\alpha_{t-1}}\Big)\mathbf{x}_{t-1}^2-2\Big(\frac{\sqrt{\alpha_t}}{\beta_t}\mathbf{x}_t+\frac{\sqrt{\bar\alpha_{t-1}}}{1-\bar\alpha_{t-1}}\mathbf{x}_0\Big)\mathbf{x}_{t-1}+\dots\Big)\Big)$$

From this formulation, we can derive that $q(\mathbf{x}_{t-1}|\mathbf{x}_t,\mathbf{x}_0)=\mathcal{N}\big(\mathbf{x}_{t-1};\tilde{\boldsymbol{\mu}}_t(\mathbf{x}_t,\mathbf{x}_0),\tilde\beta_t\boldsymbol{I}\big)$ for

$$\tilde\beta_t = 1/\Big(\frac{\alpha_t}{\beta_t}+\frac{1}{1-\bar\alpha_{t-1}}\Big) = 1/\Big(\frac{\alpha_t(1-\bar\alpha_{t-1})+\beta_t}{\beta_t(1-\bar\alpha_{t-1})}\Big) = 1/\Big(\frac{\alpha_t+\beta_t-\bar\alpha_t}{\beta_t(1-\bar\alpha_{t-1})}\Big) = \frac{1-\bar\alpha_{t-1}}{1-\bar\alpha_t}\beta_t,$$

$$\tilde{\boldsymbol{\mu}}_t(\mathbf{x}_t,\mathbf{x}_0) = \Big(\frac{\sqrt{\alpha_t}}{\beta_t}\mathbf{x}_t+\frac{\sqrt{\bar\alpha_{t-1}}}{1-\bar\alpha_{t-1}}\mathbf{x}_0\Big)\frac{1-\bar\alpha_{t-1}}{1-\bar\alpha_t}\beta_t = \frac{\sqrt{\bar\alpha_{t-1}}\beta_t}{1-\bar\alpha_t}\mathbf{x}_0+\frac{\sqrt{\alpha_t}(1-\bar\alpha_{t-1})}{1-\bar\alpha_t}\mathbf{x}_t.$$

DDPM – Loss

The full derivation of the loss is available in the Bonus Content of this presentation. The resulting loss is

$$L_t = \mathbb{E}\left[\frac{1}{2\|\sigma_t \boldsymbol{I}\|^2}\left\|\tilde{\boldsymbol{\mu}}_t(\mathbf{x}_t, \mathbf{x}_0) - \boldsymbol{\mu}_{\boldsymbol{\theta}}(\mathbf{x}_t, t)\right\|^2\right].$$

The model is then changed to predict $\boldsymbol{\varepsilon}_{\boldsymbol{\theta}}(\mathbf{x}_t, t)$ instead of $\boldsymbol{\mu}_{\boldsymbol{\theta}}(\mathbf{x}_t, t)$. The loss then becomes

$$L_t = \mathbb{E}\left[\frac{(1-\alpha_t)^2}{2\alpha_t(1-\bar{\alpha}_t)\|\sigma_t \boldsymbol{I}\|^2}\left\|\mathbf{e}_t - \boldsymbol{\varepsilon}_{\boldsymbol{\theta}}\left(\sqrt{\bar{\alpha}_t}\mathbf{x}_0 + \sqrt{1-\bar{\alpha}_t}\mathbf{e}_t, t\right)\right\|^2\right].$$

The authors found that training without the weighting term performs better, so the final loss is

$$L_t^{\text{simple}} = \mathbb{E}_{t\in\{1..T\},\mathbf{x}_0,\mathbf{e}_t}\left[\left\|\mathbf{e}_t - \boldsymbol{\varepsilon}_{\boldsymbol{\theta}}\left(\sqrt{\bar{\alpha}_t}\mathbf{x}_0 + \sqrt{1-\bar{\alpha}_t}\mathbf{e}_t, t\right)\right\|^2\right].$$

Note that both losses have the same optimum if we used independent $\boldsymbol{\varepsilon}_{\boldsymbol{\theta}_t}$ for every t.

DDPM – Training and Sampling Algorithms

Algorithm 1 Training

1: **repeat**
2: $\mathbf{x}_0 \sim q(\mathbf{x}_0)$
3: $t \sim \text{Uniform}(\{1, \dots, T\})$
4: $\boldsymbol{\epsilon} \sim \mathcal{N}(\mathbf{0}, \mathbf{I})$
5: Take gradient descent step on
$$\nabla_\theta \left\| \boldsymbol{\epsilon} - \boldsymbol{\epsilon}_\theta(\sqrt{\bar{\alpha}_t}\mathbf{x}_0 + \sqrt{1-\bar{\alpha}_t}\boldsymbol{\epsilon}, t) \right\|^2$$
6: **until** converged

Algorithm 2 Sampling

1: $\mathbf{x}_T \sim \mathcal{N}(\mathbf{0}, \mathbf{I})$
2: **for** $t = T, \dots, 1$ **do**
3: $\mathbf{z} \sim \mathcal{N}(\mathbf{0}, \mathbf{I})$ if $t > 1$, else $\mathbf{z} = \mathbf{0}$
4: $\mathbf{x}_{t-1} = \frac{1}{\sqrt{\alpha_t}} \left(\mathbf{x}_t - \frac{1-\alpha_t}{\sqrt{1-\bar{\alpha}_t}} \boldsymbol{\epsilon}_\theta(\mathbf{x}_t, t) \right) + \sigma_t \mathbf{z}$
5: **end for**
6: **return** $\mathbf{x}_0$

Algorithms 1, 2 of "Denoising Diffusion Probabilistic Models", https://arxiv.org/abs/2006.11239

In practice, instead of discrete, t may be continuous in the $[0, 1]$ range. Note that sampling using the proposed algorithm is slow because it is common to use $T = 1000$ steps during sampling.

The value of σ_t^2 is chosen to be either β_t or $\tilde{\beta}_t$, or any value in between (it can be proven that these values correspond to upper and lower bounds on the reverse process entropy).

Both of these issues are alleviated by using a different sampling algorithm DDIM, which runs in several tens of steps and does not use σ_t^2.

Stable Diffusion – Semantic and Perceptual Compression

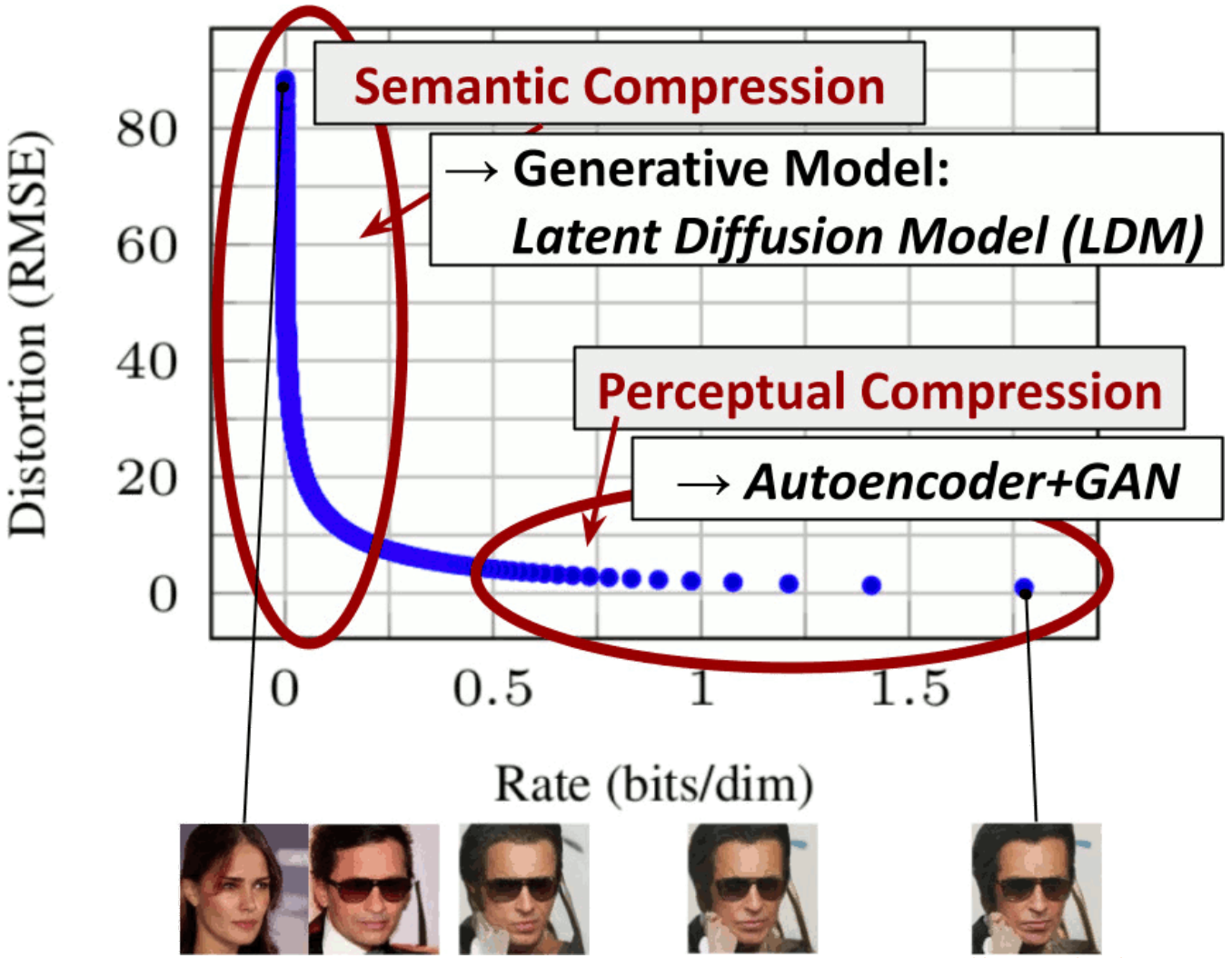

Figure 2 of "High-Resolution Image Synthesis with Latent Diffusion Models", https://arxiv.org/abs/2112.10752

Stable Diffusion – Architecture

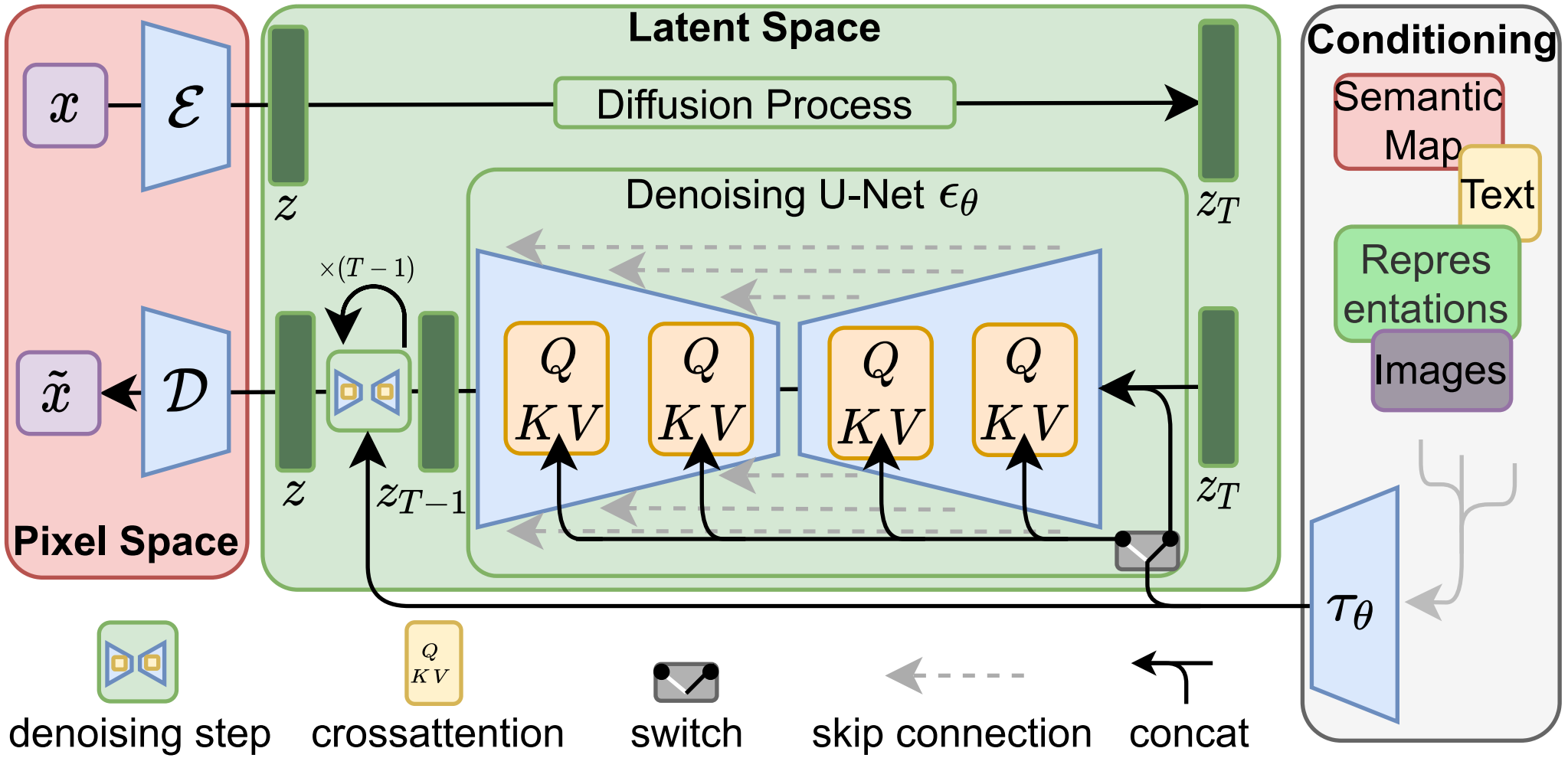

Figure 3 of "High-Resolution Image Synthesis with Latent Diffusion Models", https://arxiv.org/abs/2112.10752

Stable Diffusion Papers

- (SD) Robin Rombach, Andreas Blattmann, Dominik Lorenz, Patrick Esser, Björn Ommer: **High-Resolution Image Synthesis with Latent Diffusion Models** https://arxiv.org/abs/2112.10752
- (SDXL) Dustin Podell, Zion English, Kyle Lacey, Andreas Blattmann, Tim Dockhorn, Jonas Müller, Joe Penna, Robin Rombach: **SDXL: Improving Latent Diffusion Models for High-Resolution Image Synthesis** https://arxiv.org/abs/2307.01952
- (SD3) Patrick Esser, Sumith Kulal, Andreas Blattmann, Rahim Entezari, Jonas Müller, Harry Saini, Yam Levi, Dominik Lorenz, Axel Sauer, Frederic Boesel, Dustin Podell, Tim Dockhorn, Zion English, Kyle Lacey, Alex Goodwin, Yannik Marek, Robin Rombach: **Scaling Rectified Flow Transformers for High-Resolution Image Synthesis** https://arxiv.org/abs/2403.03206
- (SD3-Turbo) Axel Sauer, Frederic Boesel, Tim Dockhorn, Andreas Blattmann, Patrick Esser, Robin Rombach: **Fast High-Resolution Image Synthesis with Latent Adversarial Diffusion Distillation** https://arxiv.org/pdf/2403.12015

Bonus Content
DDPM Loss

DDPM – Deriving Loss using Jensen's Inequality

$$
\begin{aligned}
-\mathbb{E}_{q(\mathbf{x}_0)}\left[\log p_{\boldsymbol{\theta}}(\mathbf{x}_0)\right] &= -\mathbb{E}_{q(\mathbf{x}_0)}\left[\log \mathbb{E}_{p_{\boldsymbol{\theta}}(\mathbf{x}_{1:T})}\left[p_{\boldsymbol{\theta}}(\mathbf{x}_0|\boldsymbol{x}_{1:T})\right]\right] \\
&= -\mathbb{E}_{q(\mathbf{x}_0)}\left[\log \mathbb{E}_{q(\mathbf{x}_{1:T}|\mathbf{x}_0)}\left[\frac{p_{\boldsymbol{\theta}}(\mathbf{x}_{0:T})}{q(\mathbf{x}_{1:T}|\mathbf{x}_0)}\right]\right] \\
&\leq -\mathbb{E}_{q(\mathbf{x}_{0:T})}\left[\log \frac{p_{\boldsymbol{\theta}}(\mathbf{x}_{0:T})}{q(\mathbf{x}_{1:T}|\mathbf{x}_0)}\right] = \mathbb{E}_{q(\mathbf{x}_{0:T})}\left[\log \frac{q(\mathbf{x}_{1:T}|\mathbf{x}_0)}{p_{\boldsymbol{\theta}}(\mathbf{x}_{0:T})}\right] \\
&= \mathbb{E}_{q(\mathbf{x}_{0:T})}\left[-\log p_{\boldsymbol{\theta}}(\mathbf{x}_T) + \sum_{t=2}^{T} \log \frac{q(\mathbf{x}_t|\mathbf{x}_{t-1})}{p_{\boldsymbol{\theta}}(\mathbf{x}_{t-1}|\mathbf{x}_t)} + \log \frac{q(\mathbf{x}_1|\mathbf{x}_0)}{p_{\boldsymbol{\theta}}(\mathbf{x}_0|\mathbf{x}_1)}\right] \\
&= \mathbb{E}_{q(\mathbf{x}_{0:T})}\left[-\log p_{\boldsymbol{\theta}}(\mathbf{x}_T) + \sum_{t=2}^{T} \log \left(\frac{q(\mathbf{x}_{t-1}|\mathbf{x}_t,\mathbf{x}_0)}{p_{\boldsymbol{\theta}}(\mathbf{x}_{t-1}|\mathbf{x}_t)} \frac{q(\mathbf{x}_t|\mathbf{x}_0)}{q(\mathbf{x}_{t-1}|\mathbf{x}_0)}\right) + \log \frac{q(\mathbf{x}_1|\mathbf{x}_0)}{p_{\boldsymbol{\theta}}(\mathbf{x}_0|\mathbf{x}_1)}\right] \\
&= \mathbb{E}_{q(\mathbf{x}_{0:T})}\left[-\log p_{\boldsymbol{\theta}}(\mathbf{x}_T) + \sum_{t=2}^{T} \log \frac{q(\mathbf{x}_{t-1}|\mathbf{x}_t,\mathbf{x}_0)}{p_{\boldsymbol{\theta}}(\mathbf{x}_{t-1}|\mathbf{x}_t)} + \log \frac{q(\mathbf{x}_T|\mathbf{x}_0)}{q(\mathbf{x}_1|\mathbf{x}_0)} + \log \frac{q(\mathbf{x}_1|\mathbf{x}_0)}{p_{\boldsymbol{\theta}}(\mathbf{x}_0|\mathbf{x}_1)}\right] \\
&= \mathbb{E}_{q(\mathbf{x}_{0:T})}\left[\log \frac{q(\mathbf{x}_T|\mathbf{x}_0)}{p_{\boldsymbol{\theta}}(\mathbf{x}_T)} + \sum_{t=2}^{T} \log \frac{q(\mathbf{x}_{t-1}|\mathbf{x}_t,\mathbf{x}_0)}{p_{\boldsymbol{\theta}}(\mathbf{x}_{t-1}|\mathbf{x}_t)} - \log p_{\boldsymbol{\theta}}(\mathbf{x}_0|\mathbf{x}_1)\right] \\
&= \mathbb{E}_{q(\mathbf{x}_{0:T})}\Bigg[\underbrace{D_{\mathrm{KL}}(q(\mathbf{x}_T|\mathbf{x}_0)\|p_{\boldsymbol{\theta}}(\mathbf{x}_T))}_{L_T} + \sum_{t=2}^{T} \underbrace{D_{\mathrm{KL}}(q(\mathbf{x}_{t-1}|\mathbf{x}_t,\mathbf{x}_0)\|p_{\boldsymbol{\theta}}(\mathbf{x}_{t-1}|\mathbf{x}_t)}_{L_t} \underbrace{- \log p_{\boldsymbol{\theta}}(\mathbf{x}_0|\mathbf{x}_1)}_{L_0}\Bigg]
\end{aligned}
$$

DDPM – Deriving Loss using Jensen's Inequality

The whole loss is therefore composed of the following components:

- $L_T = D_{\mathrm{KL}}\big(q(\mathbf{x}_T|\mathbf{x}_0)\|p_{\boldsymbol{\theta}}(\mathbf{x}_T)\big)$ is constant with respect to $\boldsymbol{\theta}$ and can be ignored,
- $L_t = D_{\mathrm{KL}}\big(q(\mathbf{x}_{t-1}|\mathbf{x}_t,\mathbf{x}_0)\|p_{\boldsymbol{\theta}}(\mathbf{x}_{t-1}|\mathbf{x}_t)\big)$ is KL divergence between two Gaussians, so it can be computed explicitly as

$$L_t = \mathbb{E}\left[\frac{1}{2\|\sigma_t \boldsymbol{I}\|^2}\left\|\tilde{\boldsymbol{\mu}}_t(\mathbf{x}_t,\mathbf{x}_0) - \boldsymbol{\mu}_{\boldsymbol{\theta}}(\mathbf{x}_t,t)\right\|^2\right],$$

- $L_0 = -\log p_{\boldsymbol{\theta}}(\mathbf{x}_0|\mathbf{x}_1)$ can be used to generate discrete $\mathbf{x}_0$ from the continuous $\mathbf{x}_1$; we will ignore it in the slides for simplicity.

DDPM – Reparametrizing Model Prediction

Recall that $q(\mathbf{x}_{t-1}|\mathbf{x}_t, \mathbf{x}_0) = \mathcal{N}\left(\mathbf{x}_{t-1}; \tilde{\boldsymbol{\mu}}_t(\mathbf{x}_t, \mathbf{x}_0), \tilde{\beta}_t \boldsymbol{I}\right)$ for

$$\tilde{\boldsymbol{\mu}}_t(\mathbf{x}_t, \mathbf{x}_0) = \frac{\sqrt{\bar{\alpha}_{t-1}}\beta_t}{1-\bar{\alpha}_t}\mathbf{x}_0 + \frac{\sqrt{\alpha_t}(1-\bar{\alpha}_{t-1})}{1-\bar{\alpha}_t}\mathbf{x}_t,$$

$$\tilde{\beta}_t = \frac{1-\bar{\alpha}_{t-1}}{1-\bar{\alpha}_t}\beta_t.$$

Because $\mathbf{x}_t = \sqrt{\bar{\alpha}_t}\mathbf{x}_0 + \sqrt{1-\bar{\alpha}_t}\mathbf{e}_t$, we get $\mathbf{x}_0 = \frac{1}{\sqrt{\bar{\alpha}_t}}\left(\mathbf{x}_t - \sqrt{1-\bar{\alpha}_t}\mathbf{e}_t\right)$.

Substituting $\mathbf{x}_0$ to $\tilde{\boldsymbol{\mu}}_t$, we get

$$\begin{aligned}
\tilde{\boldsymbol{\mu}}_t(\mathbf{x}_t, \mathbf{x}_0) &= \frac{\sqrt{\bar{\alpha}_{t-1}}\beta_t}{1-\bar{\alpha}_t}\frac{1}{\sqrt{\bar{\alpha}_t}}\left(\mathbf{x}_t - \sqrt{1-\bar{\alpha}_t}\mathbf{e}_t\right) + \frac{\sqrt{\alpha_t}(1-\bar{\alpha}_{t-1})}{1-\bar{\alpha}_t}\mathbf{x}_t \\
&= \left(\frac{\sqrt{\bar{\alpha}_{t-1}}\beta_t}{1-\bar{\alpha}_t}\frac{1}{\sqrt{\bar{\alpha}_t}} + \frac{\sqrt{\alpha_t}(1-\bar{\alpha}_{t-1})}{1-\bar{\alpha}_t}\right)\mathbf{x}_t - \left(\frac{\sqrt{\bar{\alpha}_{t-1}}\beta_t}{1-\bar{\alpha}_t}\frac{\sqrt{1-\bar{\alpha}_t}}{\sqrt{\bar{\alpha}_t}}\right)\mathbf{e}_t \\
&= \frac{\beta_t + \alpha_t(1-\bar{\alpha}_{t-1})}{(1-\bar{\alpha}_t)\sqrt{\alpha_t}}\mathbf{x}_t - \left(\frac{\beta_t}{\sqrt{1-\bar{\alpha}_t}\sqrt{\alpha_t}}\right)\mathbf{e}_t = \frac{1}{\sqrt{\alpha_t}}\left(\mathbf{x}_t - \frac{1-\alpha_t}{\sqrt{1-\bar{\alpha}_t}}\mathbf{e}_t\right).
\end{aligned}$$

DDPM – Reparametrizing Model Prediction

We change our model to predict $\boldsymbol{\varepsilon_\theta}(\mathbf{x}_t, t)$ instead of $\boldsymbol{\mu_\theta}(\mathbf{x}_t, t)$. The loss L_t then becomes

$$\begin{aligned}
L_t &= \mathbb{E}\left[\frac{1}{2\|\sigma_t \boldsymbol{I}\|^2}\left\|\tilde{\boldsymbol{\mu}}_t(\mathbf{x}_t, \mathbf{x}_0) - \boldsymbol{\mu_\theta}(\mathbf{x}_t, t)\right\|^2\right] \\
&= \mathbb{E}\left[\frac{1}{2\|\sigma_t \boldsymbol{I}\|^2}\left\|\frac{1}{\sqrt{\alpha_t}}\left(\mathbf{x}_t - \frac{1-\alpha_t}{\sqrt{1-\bar{\alpha}_t}}\mathbf{e}_t\right) - \frac{1}{\sqrt{\alpha_t}}\left(\mathbf{x}_t - \frac{1-\alpha_t}{\sqrt{1-\bar{\alpha}_t}}\boldsymbol{\varepsilon_\theta}(\mathbf{x}_t, t)\right)\right\|^2\right] \\
&= \mathbb{E}\left[\frac{(1-\alpha_t)^2}{2\alpha_t(1-\bar{\alpha}_t)\|\sigma_t \boldsymbol{I}\|^2}\left\|\mathbf{e}_t - \boldsymbol{\varepsilon_\theta}(\mathbf{x}_t, t)\right\|^2\right] \\
&= \mathbb{E}\left[\frac{(1-\alpha_t)^2}{2\alpha_t(1-\bar{\alpha}_t)\|\sigma_t \boldsymbol{I}\|^2}\left\|\mathbf{e}_t - \boldsymbol{\varepsilon_\theta}\left(\sqrt{\bar{\alpha}_t}\mathbf{x}_0 + \sqrt{1-\bar{\alpha}_t}\mathbf{e}_t, t\right)\right\|^2\right].
\end{aligned}$$

The authors found that training without the weighting term performs better, so the final loss is

$$L_t^{\text{simple}} = \mathbb{E}_{t\in\{1..T\},\mathbf{x}_0,\mathbf{e}_t}\left[\left\|\mathbf{e}_t - \boldsymbol{\varepsilon_\theta}\left(\sqrt{\bar{\alpha}_t}\mathbf{x}_0 + \sqrt{1-\bar{\alpha}_t}\mathbf{e}_t, t\right)\right\|^2\right].$$

Note that both losses have the same optimum if we used independent $\boldsymbol{\varepsilon}_{\boldsymbol{\theta}_t}$ for every t.

Bonus Content
DDIM Sampling

Denoising Diffusion Implicit Models

We now describe *Denoising Diffusion Implicit Models (DDIM)*, which utilize a different forward process.

This forward process is designed to:

- allow faster sampling,
- have the same "marginals" $q(\mathbf{x}_t|\mathbf{x}_0) = \mathcal{N}\left(\sqrt{\bar{\alpha}_t}\mathbf{x}_0, (1-\bar{\alpha}_t)\boldsymbol{I}\right)$.

The second condition will allow us to use the same loss as in DDPM; therefore, the training algorithm is exactly identical do DDPM, only the sampling algorithm is different.

Note that in the slides, only a special case of DDIM is described; the original paper describes a more general forward process. However, the special case presented here is almost exclusively used.

Denoising Diffusion Implicit Models – The Forward Process

The forward process of DDIM can be described using

$$q_0(\mathbf{x}_{1:T}|\mathbf{x}_0) = q_0(\mathbf{x}_T|\mathbf{x}_0)\prod_{t=2}^{T} q_0(\mathbf{x}_{t-1}|\mathbf{x}_t,\mathbf{x}_0),$$

where

- $q_0(\mathbf{x}_T|\mathbf{x}_0) = \mathcal{N}\left(\sqrt{\bar{\alpha}_T}\mathbf{x}_0, (1-\bar{\alpha}_T)\boldsymbol{I}\right)$,
- $q_0(\mathbf{x}_{t-1}|\mathbf{x}_t,\mathbf{x}_0) = \mathcal{N}\left(\sqrt{\bar{\alpha}_{t-1}}\mathbf{x}_0 + \sqrt{1-\bar{\alpha}_{t-1}}\left(\frac{\mathbf{x}_t-\sqrt{\bar{\alpha}_t}\mathbf{x}_0}{\sqrt{1-\bar{\alpha}_t}}\right), 0\cdot\boldsymbol{I}\right)$.

With these definitions, we can prove by induction that $q_0(\mathbf{x}_t|\mathbf{x}_0) = \mathcal{N}\left(\sqrt{\bar{\alpha}_t}\mathbf{x}_0, (1-\bar{\alpha}_t)\boldsymbol{I}\right)$:

$$\begin{aligned}\mathbf{x}_{t-1} &= \sqrt{\bar{\alpha}_{t-1}}\mathbf{x}_0 + \sqrt{1-\bar{\alpha}_{t-1}}\left(\frac{\mathbf{x}_t-\sqrt{\bar{\alpha}_t}\mathbf{x}_0}{\sqrt{1-\bar{\alpha}_t}}\right)\\ &= \sqrt{\bar{\alpha}_{t-1}}\mathbf{x}_0 + \sqrt{1-\bar{\alpha}_{t-1}}\left(\frac{\sqrt{\bar{\alpha}_t}\mathbf{x}_0+\sqrt{1-\bar{\alpha}_t}\mathbf{e}_t-\sqrt{\bar{\alpha}_t}\mathbf{x}_0}{\sqrt{1-\bar{\alpha}_t}}\right) = \sqrt{\bar{\alpha}_{t-1}}\mathbf{x}_0 + \sqrt{1-\bar{\alpha}_{t-1}}\mathbf{e}_t.\end{aligned}$$

The real "forward" $q_0(\mathbf{x}_t|\mathbf{x}_{t-1},\mathbf{x}_0)$ can be expressed using Bayes' theorem using the above definition, but we do not actually need it.

Denoising Diffusion Implicit Models – The Reverse Process

The definition of $q_0(\mathbf{x}_{t-1}|\mathbf{x}_t, \mathbf{x}_0)$ provides us also with a sampling algorithm; after sampling the initial noise $\mathbf{x}_T \sim \mathcal{N}(\mathbf{0}, \boldsymbol{I})$, we perform the following for t from T down to 1:

$$\begin{aligned}\boldsymbol{x}_{t-1} &= \sqrt{\bar{\alpha}_{t-1}}\mathbf{x}_0 + \sqrt{1-\bar{\alpha}_{t-1}}\boldsymbol{\varepsilon}_{\boldsymbol{\theta}}(\boldsymbol{x}_t, t) \\ &= \sqrt{\bar{\alpha}_{t-1}}\left(\frac{\boldsymbol{x}_t - \sqrt{1-\bar{\alpha}_t}\boldsymbol{\varepsilon}_{\boldsymbol{\theta}}(\boldsymbol{x}_t,t)}{\sqrt{\bar{\alpha}_t}}\right) + \sqrt{1-\bar{\alpha}_{t-1}}\boldsymbol{\varepsilon}_{\boldsymbol{\theta}}(\boldsymbol{x}_t, t).\end{aligned}$$

An important property of q_0 is that it can also model several steps at once:

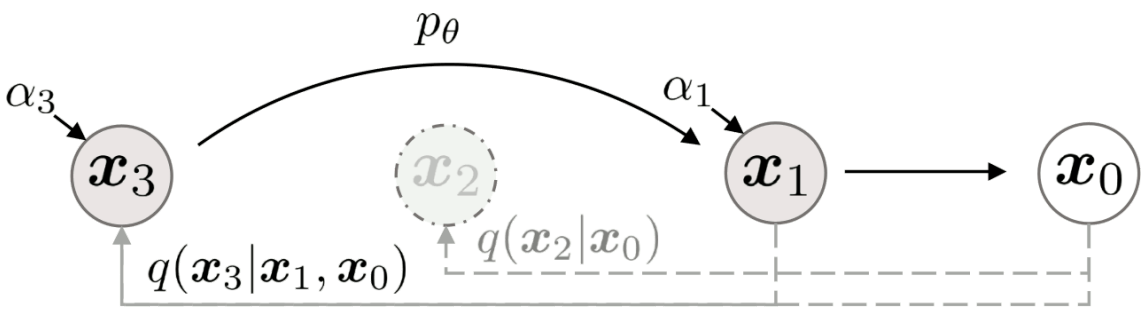

Figure 2 of "Denoising Diffusion Implicit Models", https://arxiv.org/abs/2010.02502

$$q_0(\mathbf{x}_{t'}|\mathbf{x}_t, \mathbf{x}_0) = \mathcal{N}\left(\sqrt{\bar{\alpha}_{t'}}\mathbf{x}_0 + \sqrt{1-\bar{\alpha}_{t'}}\left(\frac{\mathbf{x}_t - \sqrt{\bar{\alpha}_t}\mathbf{x}_0}{\sqrt{1-\bar{\alpha}_t}}\right), \mathbf{0}\right).$$

Denoising Diffusion Implicit Models – Accelerated Sampling

We base our accelerated sampling algorithm on the "multistep" $q_0(\mathbf{x}_{t'} | \mathbf{x}_t, \mathbf{x}_0)$.

Let $t_S = T, t_{S-1}, \ldots, t_1$ be a subsequence of the process steps (usually, a uniform subsequence of $T, \ldots, 1$ is used), and let $t_0 = 0$. Starting from initial noise $\mathbf{x}_T \sim \mathcal{N}(\mathbf{0}, \boldsymbol{I})$, we perform S sampling steps for i from S down to 1:

$$\boldsymbol{x}_{t_{i-1}} \leftarrow \sqrt{\bar{\alpha}_{t_{i-1}}} \underbrace{\left(\frac{\boldsymbol{x}_{t_i} - \sqrt{1-\bar{\alpha}_{t_i}}\, \boldsymbol{\varepsilon}_{\boldsymbol{\theta}}(\boldsymbol{x}_{t_i}, t_i)}{\sqrt{\bar{\alpha}_{t_i}}} \right)}_{\boldsymbol{x}_0 \text{ estimate}} + \sqrt{1 - \bar{\alpha}_{t_{i-1}}}\, \boldsymbol{\varepsilon}_{\boldsymbol{\theta}}(\boldsymbol{x}_{t_i}, t_i).$$

The sampling procedure can be described in words as follows:

- using the current time step t_i, we compute the estimated noise $\boldsymbol{\varepsilon}_{\boldsymbol{\theta}}(\boldsymbol{x}_{t_i}, t_i)$;
- by utilizing the current signal rate $\sqrt{\bar{\alpha}_{t_i}}$ and noise rate $\sqrt{1 - \bar{\alpha}_{t_i}}$, we estimate $\mathbf{x}_0$;
- we obtain $\boldsymbol{x}_{t_{i-1}}$ by combining the estimated signal $\mathbf{x}_0$ and noise $\boldsymbol{\varepsilon}_{\boldsymbol{\theta}}(\boldsymbol{x}_{t_i}, t_i)$ using the signal and noise rates of the time step t_{i-1}.

For comparison, we show both the original DDPM and the new DDIM sampling algorithms:

- sample $\boldsymbol{x}_T$ from $\mathcal{N}(\mathbf{0}, \boldsymbol{I})$
- let $t_S = T, t_{S-1}, \ldots, t_1 = 1$ be a subsequence of the process steps
  - DDPM: the original sequence $T, \ldots, 1$ is usually used
  - DDIM: S regularly-spaced steps T, $\frac{S-1}{S}T$, $\frac{S-2}{S}T, \ldots, 1$ are usually used
  - additionally, we define $t_0 = 0$
- for $i = S, \ldots, 1$:

$$\text{DDPM}: \quad \boldsymbol{x}_{t_{i-1}} \leftarrow \sqrt{\frac{1}{\alpha_{t_i}}}\left(\boldsymbol{x}_{t_i} - \frac{1-\alpha_{t_i}}{\sqrt{1-\bar{\alpha}_{t_i}}}\boldsymbol{\varepsilon}_{\boldsymbol{\theta}}(\boldsymbol{x}_{t_i}, t_i)\right) + \sigma_t \boldsymbol{z}_t$$

$$\text{DDIM}: \quad \boldsymbol{x}_{t_{i-1}} \leftarrow \sqrt{\bar{\alpha}_{t_{i-1}}}\underbrace{\left(\frac{\boldsymbol{x}_{t_i} - \sqrt{1-\bar{\alpha}_{t_i}}\boldsymbol{\varepsilon}_{\boldsymbol{\theta}}(\boldsymbol{x}_{t_i}, t_i)}{\sqrt{\bar{\alpha}_{t_i}}}\right)}_{\boldsymbol{x}_0 \text{ estimate}} + \sqrt{1-\bar{\alpha}_{t_{i-1}}}\boldsymbol{\varepsilon}_{\boldsymbol{\theta}}(\boldsymbol{x}_{t_i}, t_i)$$

- return $\boldsymbol{x}_0$

DDIM – Accelerated Sampling Examples

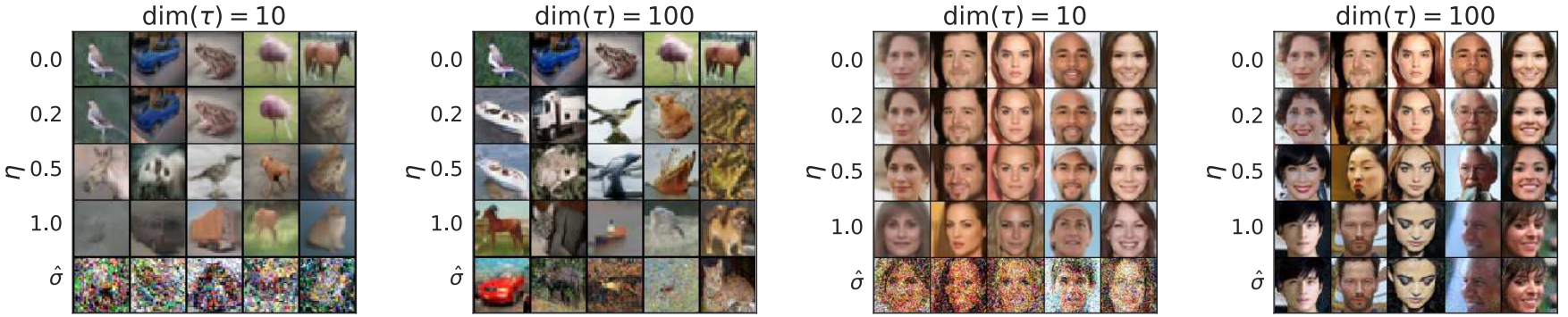

Figure 3 of "Denoising Diffusion Implicit Models", https://arxiv.org/abs/2010.02502

Figure 5 of "Denoising Diffusion Implicit Models", https://arxiv.org/abs/2010.02502

Bonus Content
Score Matching

Score Matching

Recall that loglikelihood-based models explicit represent the density function, commonly using an unnormalized probabilistic model

$$p_{\boldsymbol{\theta}}(\mathbf{x}) = \frac{e^{f_{\boldsymbol{\theta}}(\mathbf{x})}}{Z_{\boldsymbol{\theta}}},$$

and it is troublesome to ensure the tractability of the normalization constant $Z_{\boldsymbol{\theta}}$.

One way how to avoid the normalization is to avoid the explicit density $p_{\boldsymbol{\theta}}(\mathbf{x})$, and represent a **score function** instead, where the score function is the gradient of the log density:

$$s_{\boldsymbol{\theta}}(\mathbf{x}) = \nabla_{\mathbf{x}} \log p_{\boldsymbol{\theta}}(\mathbf{x}),$$

because

$$s_{\boldsymbol{\theta}}(\mathbf{x}) = \nabla_{\mathbf{x}} \log p_{\boldsymbol{\theta}}(\mathbf{x}) = \nabla_{\mathbf{x}} \log \frac{e^{f_{\boldsymbol{\theta}}(\mathbf{x})}}{Z_{\boldsymbol{\theta}}} = \nabla_{\mathbf{x}} f_{\boldsymbol{\theta}}(\mathbf{x}) - \underbrace{\nabla_{\mathbf{x}} \log Z_{\boldsymbol{\theta}}}_{0} = \nabla_{\mathbf{x}} f_{\boldsymbol{\theta}}(\mathbf{x}).$$

Langevin Dynamics

When we have a score function $\nabla_{\mathbf{x}} \log p_{\boldsymbol{\theta}}(\mathbf{x})$, we can use it to perform sampling from the distribution $p_{\boldsymbol{\theta}}(\mathbf{x})$ by using **Langevin dynamics**, which is an algorithm akin to SGD, but performing sampling instead of optimum finding. Starting with $\mathbf{x}_0$, we iteratively set

$$\mathbf{x}_{i+1} \leftarrow \mathbf{x}_i + \varepsilon \nabla_{\mathbf{x}_i} \log p_{\boldsymbol{\theta}}(\mathbf{x}_i) + \sqrt{2\varepsilon}\, \mathbf{z}_i, \quad \text{where } \boldsymbol{z}_i \sim \mathcal{N}(\mathbf{0}, \boldsymbol{I}).$$

When $\varepsilon \to 0$ and $K \to \infty$, $\mathbf{x}_K$ obtained by the Langevin dynamics converges to a sample from the distribution $p_{\boldsymbol{\theta}}(\mathbf{x})$.

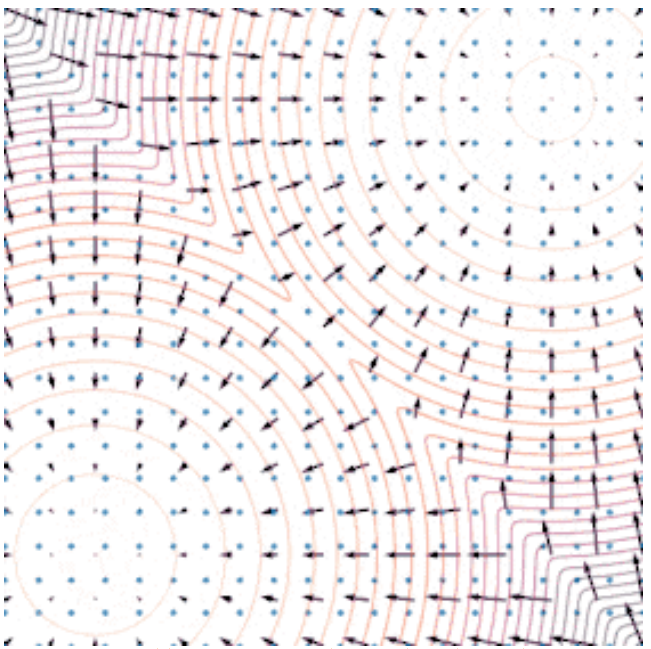

https://yang-song.net/assets/img/score/langevin.gif

Score-Based Generative Modeling

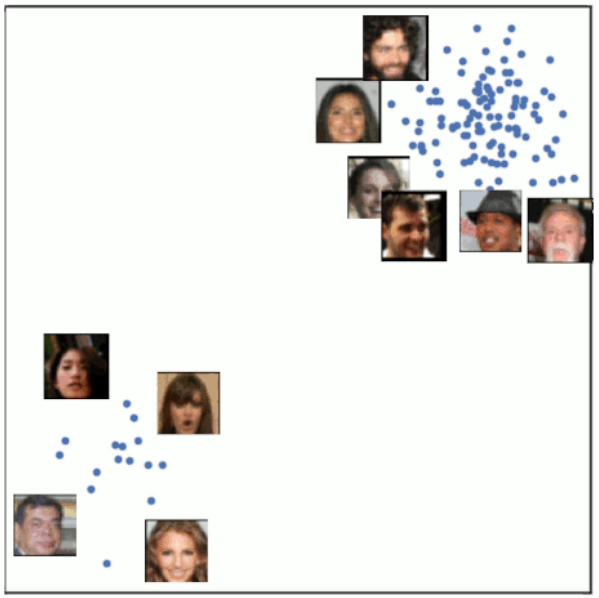

Data samples

$$\{\mathbf{x}_1, \mathbf{x}_2, \cdots, \mathbf{x}_N\} \overset{\text{i.i.d.}}{\sim} p(\mathbf{x})$$

score matching

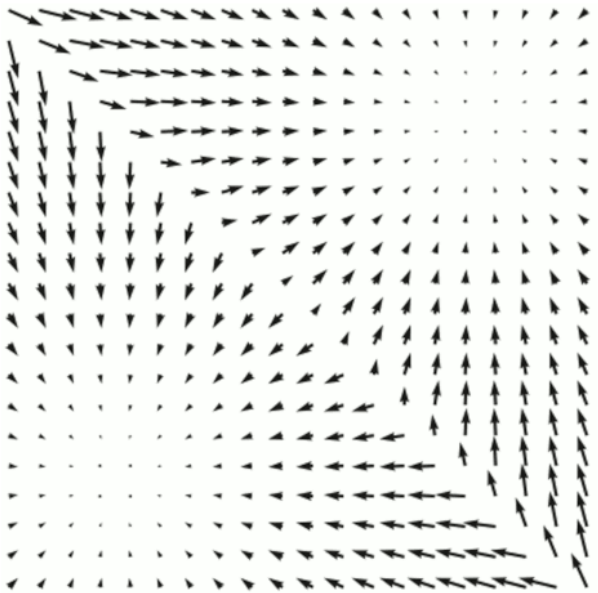

Scores

$$\mathbf{s}_\theta(\mathbf{x}) \approx \nabla_{\mathbf{x}} \log p(\mathbf{x})$$

Langevin dynamics

New samples

https://yang-song.net/assets/img/score/smld.jpg

Noise Conditional Score Network

However, estimating the score function from data is inaccurate in low-density regions.

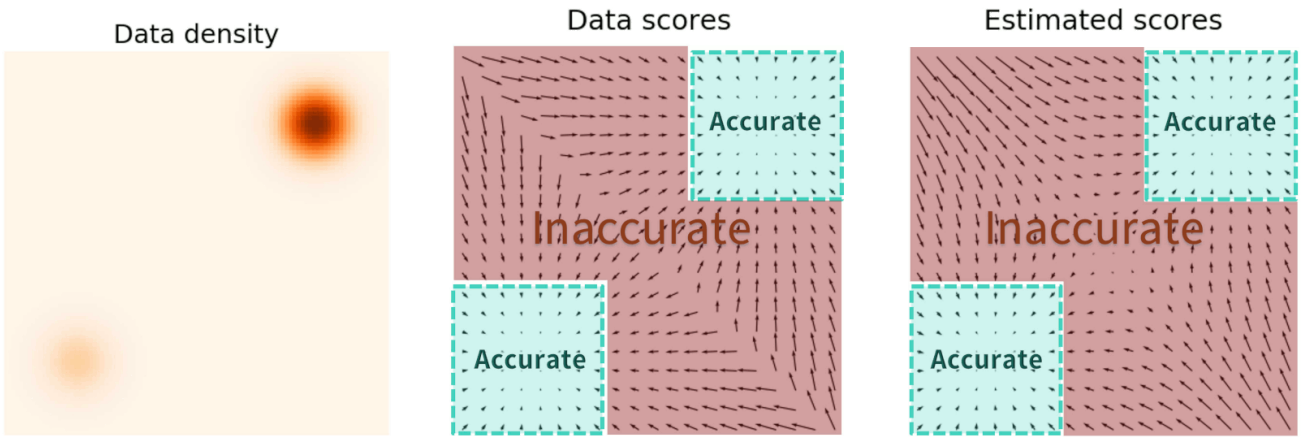

https://yang-song.net/assets/img/score/pitfalls.jpg

In order to accurately estimate the score function in low-density regions, we perturb the data distribution by isotropic Gaussian noise with various noise rates σ_t:

$$q_{\sigma_t}(\tilde{\mathbf{x}}) \stackrel{\text{def}}{=} \mathbb{E}_{\mathbf{x}\sim p(\mathbf{x})}\left[\mathcal{N}(\tilde{\mathbf{x}}; \mathbf{x}, {\sigma_t}^2 \boldsymbol{I})\right],$$

where the noise distribution $q_{\sigma_t}(\tilde{\mathbf{x}}|\mathbf{x}) = \mathcal{N}(\tilde{\mathbf{x}}; \mathbf{x}, \sigma_t^2 \boldsymbol{I})$ as analogous to the forward process in the diffusion models.

Noise Conditional Score Network

To train the score function $\boldsymbol{s}_{\boldsymbol{\theta}}(\mathbf{x}, \sigma_t) = \nabla_{\mathbf{x}} \log q_{\sigma_t}(\mathbf{x})$, we need to minimize the following objective:

$$\mathbb{E}_{t, \tilde{\mathbf{x}} \sim q_{\sigma_t}} \left[\left\| \boldsymbol{s}_{\boldsymbol{\theta}}(\tilde{\mathbf{x}}, \sigma_t) - \nabla_{\tilde{\mathbf{x}}} \log q_{\sigma_t}(\tilde{\mathbf{x}}) \right\|^2 \right].$$

It can be shown (see *P. Vincent: A connection between score matching and denoising autoencoders*) that it is equivalent to minimize the *denoising score matching* objective:

$$\mathbb{E}_{t, \mathbf{x} \sim p(\mathbf{x}), \tilde{\mathbf{x}} \sim q_{\sigma_t}(\tilde{\mathbf{x}}|\mathbf{x})} \left[\left\| \boldsymbol{s}_{\boldsymbol{\theta}}(\tilde{\mathbf{x}}, \sigma_t) - \nabla_{\tilde{\boldsymbol{x}}} \log q_{\sigma_t}(\tilde{\mathbf{x}}|\mathbf{x}) \right\|^2 \right].$$

In our case, $\nabla_{\tilde{\mathbf{x}}} \log q_{\sigma_t}(\tilde{\mathbf{x}}|\mathbf{x}) = \nabla_{\tilde{\mathbf{x}}} \frac{-\|\tilde{\mathbf{x}}-\mathbf{x}\|^2}{2\sigma_t^2} = -\frac{\tilde{\mathbf{x}}-\mathbf{x}}{\sigma_t^2}$. Because $\tilde{\mathbf{x}} = \mathbf{x} + \sigma_t \mathbf{e}$ for standard normal random variable $\mathbf{e} \sim \mathcal{N}(\mathbf{0}, \boldsymbol{I})$, we can rewrite the objective to

$$\mathbb{E}_{t, \mathbf{x} \sim p(\mathbf{x}), \mathbf{e} \sim \mathcal{N}(\mathbf{0}, \boldsymbol{I})} \left[\left\| \boldsymbol{s}_{\boldsymbol{\theta}}(\mathbf{x} + \sigma_t \mathbf{e}, \sigma_t) - \frac{-\mathbf{e}}{\sigma_t} \right\|^2 \right],$$

so the score function basically estimates the noise given a noised image.

Noise Conditional Score Network

Once we have trained the score function for various noise rates σ_t, we can sample using annealed Langevin dynamics, where we utilize using gradually smaller noise rates σ_t.

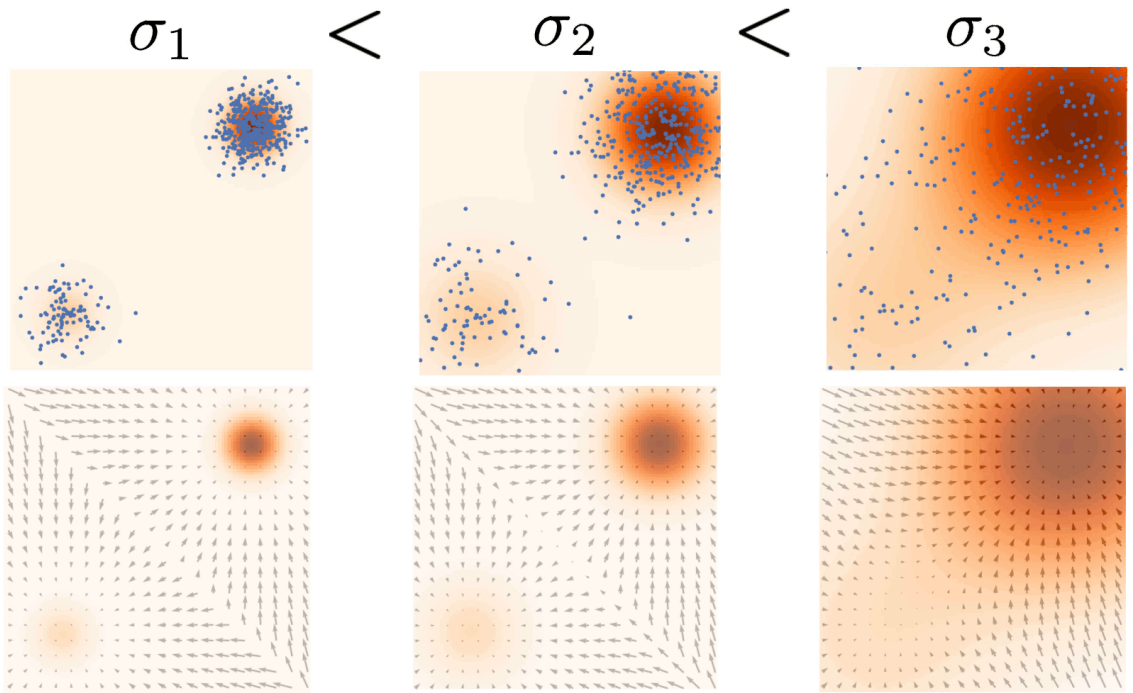

https://yang-song.net/assets/img/score/multi_scale.jpg

Algorithm 1 Annealed Langevin dynamics.

Require: $\{\sigma_i\}_{i=1}^{L}, \epsilon, T$.

Initialize $\tilde{\mathbf{x}}_0$
for $i \leftarrow 1$ to L **do**
  $\alpha_i \leftarrow \epsilon \cdot \sigma_i^2/\sigma_L^2$ ▷ α_i is the step size.
  for $t \leftarrow 1$ to T **do**
    Draw $\mathbf{z}_t \sim \mathcal{N}(0, I)$
    $\tilde{\mathbf{x}}_t \leftarrow \tilde{\mathbf{x}}_{t-1} + \frac{\alpha_i}{2}\mathbf{s}_{\boldsymbol{\theta}}(\tilde{\mathbf{x}}_{t-1}, \sigma_i) + \sqrt{\alpha_i}\,\mathbf{z}_t$
  end for
  $\tilde{\mathbf{x}}_0 \leftarrow \tilde{\mathbf{x}}_T$
end for
return $\tilde{\mathbf{x}}_T$

Algorithm 1 of "Generative Modeling by Estimating Gradients of the Data Distribution", https://arxiv.org/abs/1907.05600

Such a procedure is reminiscent to the reverse diffusion process sampling.

Bonus Content
Further Reading

Development of GANs

- Martin Arjovsky, Soumith Chintala, Léon Bottou: **Wasserstein GAN** https://arxiv.org/abs/1701.07875
- Ishaan Gulrajani, Faruk Ahmed, Martin Arjovsky, Vincent Dumoulin, Aaron Courville: **Improved Training of Wasserstein GANs** https://arxiv.org/abs/1704.00028
- Tero Karras, Timo Aila, Samuli Laine, Jaakko Lehtinen: **Progressive Growing of GANs for Improved Quality, Stability, and Variation** https://arxiv.org/abs/1710.10196
- Takeru Miyato, Toshiki Kataoka, Masanori Koyama, Yuichi Yoshida: **Spectral Normalization for Generative Adversarial Networks** https://arxiv.org/abs/1802.05957
- Zhiming Zhou, Yuxuan Song, Lantao Yu, Hongwei Wang, Jiadong Liang, Weinan Zhang, Zhihua Zhang, Yong Yu: **Understanding the Effectiveness of Lipschitz-Continuity in Generative Adversarial Nets** https://arxiv.org/abs/1807.00751
- Andrew Brock, Jeff Donahue, Karen Simonyan: **Large Scale GAN Training for High Fidelity Natural Image Synthesis** https://arxiv.org/abs/1809.11096
- Tero Karras, Samuli Laine, Timo Aila: **A Style-Based Generator Architecture for Generative Adversarial Networks** https://arxiv.org/abs/1812.04948

BigGAN

Figure 1 of "Large Scale GAN Training for High Fidelity Natural Image Synthesis", https://arxiv.org/abs/1809.11096

Figure 2 of "Large Scale GAN Training for High Fidelity Natural Image Synthesis", https://arxiv.org/abs/1809.11096

BigGAN

Figure 7 of "Large Scale GAN Training for High Fidelity Natural Image Synthesis", https://arxiv.org/abs/1809.11096

Development of VAEs

- Aaron van den Oord, Oriol Vinyals, Koray Kavukcuoglu: **Neural Discrete Representation Learning** https://arxiv.org/abs/1711.00937
- Ali Razavi, Aaron van den Oord, Oriol Vinyals: **Generating Diverse High-Fidelity Images with VQ-VAE-2** https://arxiv.org/abs/1906.00446
- Patrick Esser, Robin Rombach, Björn Ommer: **Taming Transformers for High-Resolution Image Synthesis** https://arxiv.org/abs/2012.09841
- Aditya Ramesh, Mikhail Pavlov, Gabriel Goh, Scott Gray, Chelsea Voss, Alec Radford, Mark Chen, Ilya Sutskever: **Zero-Shot Text-to-Image Generation** https://arxiv.org/abs/2102.12092
- Robin Rombach, Andreas Blattmann, Dominik Lorenz, Patrick Esser, Björn Ommer: **High-Resolution Image Synthesis with Latent Diffusion Models** https://arxiv.org/abs/2112.10752

Development of Diffusion Models

- Yang Song, Stefano Ermon: **Generative Modeling by Estimating Gradients of the Data Distribution** https://arxiv.org/abs/1907.05600
- Jonathan Ho, Ajay Jain, Pieter Abbeel: **Denoising Diffusion Probabilistic Models** https://arxiv.org/abs/2006.11239
- Jiaming Song, Chenlin Meng, Stefano Ermon: **Denoising Diffusion Implicit Models** https://arxiv.org/abs/2010.02502
- Alex Nichol, Prafulla Dhariwal: **Improved Denoising Diffusion Probabilistic Models** https://arxiv.org/abs/2102.09672
- Prafulla Dhariwal, Alex Nichol: **Diffusion Models Beat GANs on Image Synthesis** https://arxiv.org/abs/2105.05233
- Robin Rombach, Andreas Blattmann, Dominik Lorenz, Patrick Esser, Björn Ommer: **High-Resolution Image Synthesis with Latent Diffusion Models** https://arxiv.org/abs/2112.10752

SR3 Super-Resolution via Diffusion

- Chitwan Saharia, Jonathan Ho, William Chan, Tim Salimans, David J. Fleet, M. Norouzi: **Image Super-Resolution via Iterative Refinement** https://arxiv.org/abs/2104.07636

Diffusion-Based Text-Conditional Image Generation

- Alex Nichol et al.: **GLIDE: Towards Photorealistic Image Generation and Editing with Text-Guided Diffusion Models** https://arxiv.org/abs/2112.10741

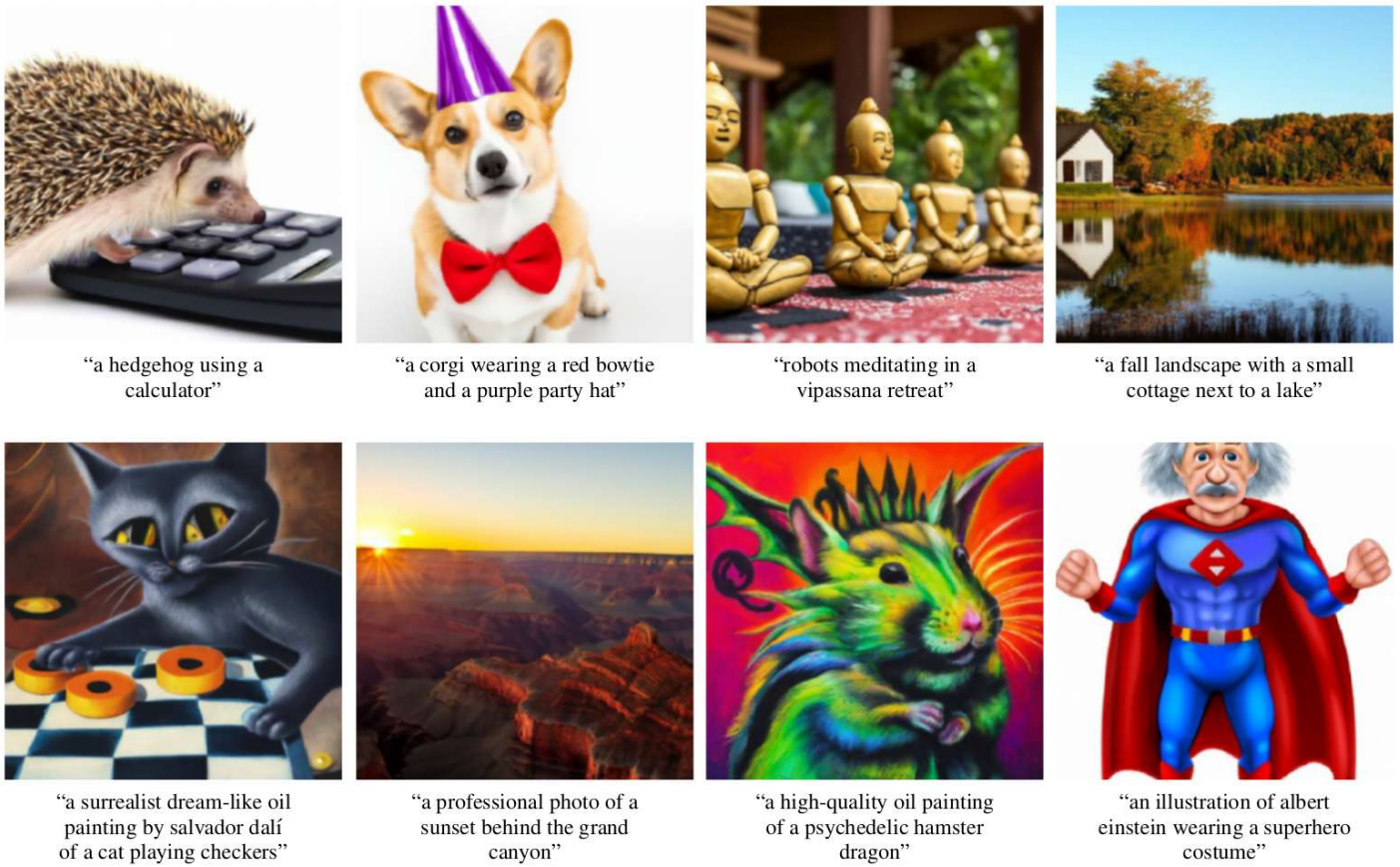

Figure 1 of "GLIDE: Towards Photorealistic Image Generation and Editing with Text-Guided Diffusion Models", https://arxiv.org/abs/2112.10741

Diffusion-Based Text-Conditional Image Generation

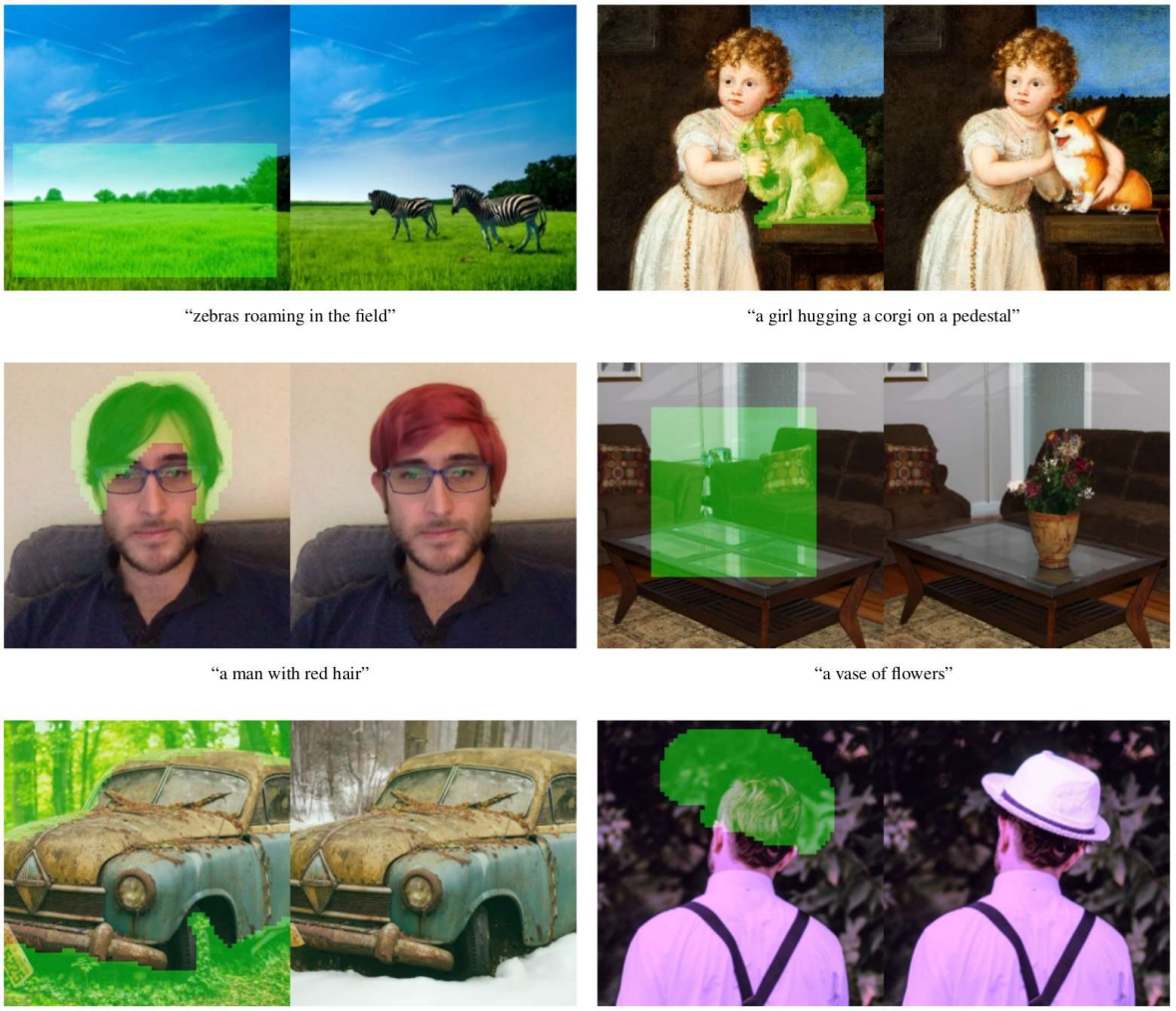

Figure 2 of "GLIDE: Towards Photorealistic Image Generation and Editing with Text-Guided Diffusion Models", https://arxiv.org/abs/2112.10741

Diffusion-Based Text-Conditional Image Generation

- Chitwan Saharia, William Chan, Saurabh Saxena, Lala Li, Jay Whang, et al.: **Photorealistic Text-to-Image Diffusion Models with Deep Language Understanding**
  https://arxiv.org/abs/2205.11487

Figure 1 of "Photorealistic Text-to-Image Diffusion Models with Deep Language Understanding", https://arxiv.org/abs/2205.11487

Normalizing Flows

- Laurent Dinh, David Krueger, Yoshua Bengio: **NICE: Non-linear Independent Components Estimation** https://arxiv.org/abs/1410.8516
- Laurent Dinh, Jascha Sohl-Dickstein, Samy Bengio: **Density estimation using Real NVP** https://arxiv.org/abs/1605.08803
- Diederik P. Kingma, Prafulla Dhariwal: **Glow: Generative Flow with Invertible 1x1 Convolutions** https://arxiv.org/abs/1807.03039

Figure 1 of "Glow: Generative Flow with Invertible 1×1 Convolutions", https://arxiv.org/abs/1807.03039